Final-state interactions and relativistic effects in the quasielastic (e,e') reaction

C. R. Chinn
Department of Physics and Astronomy, University of Maryland, College Park, Maryland 20742
and Physics Division, Los Alamos National Laboratory, Los Alamos, New Mexico 87545

A. Picklesimer
Physics Division, Los Alamos National Laboratory, Los Alamos, New Mexico 87545

J. W. Van Orden
Continuous Electron Beam Accelerator Facility, Newport News, Virginia 23606
(Received 16 December 1988)

The longitudinal and transverse response functions for the inclusive quasielastic (e,e') reaction are analyzed in detail. A microscopic theoretical framework for the many-body reaction provides a clear conceptual (nonrelativistic) basis for treating final-state interactions and goes far beyond simple plane-wave or Hermitean potential models. The many-body physics of inelastic final-state channels as described by optical and multiple scattering theories is properly included by incorporating a full complex optical potential. Explicit nonrelativistic and relativistic momentum-space calculations quantitatively demonstrate the importance of such a treatment of final-state interactions for both the transverse and longitudinal response. Nonrelativistic calculations are performed using final-state interactions based on phenomenology, local density models, and microscopic multiple scattering theory. Relativistic calculations span a similar range of models and employ Dirac bound-state wave functions. The theoretical extension to relativistic dynamics is of course not clear, but is done in obvious parallel to elastic proton scattering. Extensive calculations are performed for ^{40}Ca at momentum transfers of 410, 550, and 700 MeV/c. A number of interesting physical effects are observed, including significant relativistic suppressions (especially for R_L), large off-shell and virtual pair effects, enhancement of the tails of the response by the final-state interactions, and large qualitative and even shape distinctions between the predictions of the various models of the final-state interactions. None of the models is found to be able to simultaneously predict the data for both response functions. This strongly suggests that additional physical mechanisms are of qualitative importance in inclusive quasielastic electron scattering.

I. INTRODUCTION

One of the major issues facing electronuclear physics is the need for a comprehensive understanding of the dynamics of quasielastic electron scattering. This is the case despite the long standing existence of a physical model of quasielastic scattering which does a remarkably good job of describing the gross features of such reactions. This misleadingly simple model effectively identifies quasielastic scattering with the direct knockout of a single nucleon from the nucleus. For the inclusive (e,e') reaction this results in a large peak in the cross section centered roughly at values of energy and momentum transfer which are associated with elastic scattering from a single nucleon at rest.[1] Any shift from this ideal position is the result of some average binding corrections and the width of the peak is associated with the Fermi motion of the nucleons in the nucleus. As long as only inclusive cross sections were measured, extremely simple models of this process, such as the Fermi gas model, provided a remarkably accurate description of the position and width of the quasielastic peak.[1,2] The only remaining problem seemed to be the description of the additional structure appearing above the quasielastic peak, which was assumed to be associated with the excitation of mesonic degrees of freedom in the nucleus. However, the fact that oversimplified models are capable of describing the gross features of the quasielastic peak does not mean that the reasons for this circumstance are understood. The really remarkable result is that such a complex physical process should be so well described by such rudimentary models.

During this decade, Rosenbluth separations of the longitudinal and transverse response functions for quasielastic (e,e') have been performed for a variety of nuclei.[3-5] These response functions display several new and interesting features, some of which have proven resistant to theoretical analysis. Anomalous structure in the cross section is present in the transverse response above the quasielastic peak, but absent in the longitudinal response.[3-5] This is not in disagreement with the supposition that this structure is the result of the excitation of pionic degrees of freedom in the nucleus, however the magnitude of the effect is at least unexpected. Although simple models of quasielastic scattering fare well in describing the position and size of the transverse response, the same models are not in accord with the observed longitudinal response.[2,4] As we will see, more sophisticated models yield disparate transverse predictions

for a reasonable range of input assumptions. The trend of these models is away from the observed transverse response, but toward the observed longitudinal response. Moreover, there exists no parameter-free prediction of the complete transverse response, particularly in the region between the quasielastic and delta-resonance peaks. Until a unified and consistent description is produced, skepticism concerning simple calculations of the transverse quasielastic response must be maintained.

The observed longitudinal response is shifted to lower energy transfers at momentum transfers below approximately 400 MeV/c, relative to the value expected for quasielastic scattering, while the transverse appears near the expected quasielastic value. This feature is suggestive of contributions from long-range correlations excited by longitudinal virtual photons. A number of calculations of the longitudinal response have been carried out in the context of the random-phase approximation (RPA) and these have been successful in providing a qualitative description of the longitudinal response at low momentum transfers.[6] These calculations also predict some additional shifts and screening effects in both response functions at momentum transfers above those where the need for such long-range correlations is obvious in the data, but at energy transfers above 400 MeV/c 1p-1h RPA effects tend to be very small.[7] With the exception of some calculations which use the second RPA (SRPA),[7–9] these calculations still conform to the simplified concept of quasielastic scattering in which a single nucleon is ejected from the nucleus.

Finally, at the largest momentum transfers for which separated response functions are available, the longitudinal response for medium-sized nuclei is significantly smaller in both overall size and in integrated area than is predicted by simple models of quasielastic (e,e') and is in apparent violation of the Coulomb sum rule.[10] This has led to a considerable amount of speculation as to the physical source of this suppression. In addition to the possible need for a better description of the many-body dynamics of this process, it has been suggested that the suppression may be due to modification of the nucleon size in the nuclear medium,[11] quark clustering effects,[12] or the result of relativistic dynamics.[13–20]

For example, a number of relativistic RPA calculations[16–20] have produced large suppressions of the longitudinal response at all values of $|\mathbf{q}|$, especially when renormalized vacuum-vacuum Dirac sea correlations are included. The magnitude of the suppression is consistent with the available data, while the suppression persists to larger momentum transfers, as is not the case in nonrelativistic RPA calculations. Although the trend of these results has the right character for explaining the apparent discrepancy between data and the more conventional calculations of similar type, it is necessary to view them with caution. The effective isoscalar field theory of Ref. 21 is used to represent the residual particle-hole interaction in these RPA calculations. It is not clear, at present, to what extent these results will persist if a more realistic representation of the N-N interaction is used. It has also recently been shown that the theory of Ref. 21 is not even qualitatively stable with respect to a loop expansion.[22] Furthermore, renormalized relativistic RPA calculations that use pointlike interactions have been shown to generate unphysical singularities at momentum transfers of a few GeV/c.[23] It is therefore necessary to ensure that the desirable behavior of these calculations is not accidental or the result of pathologies.

Clearly, before appealing to these more exotic suggestions, it is necessary to reconsider the basic assumptions of simple models of quasielastic scattering and to seriously address the many-body nature of the reaction. The major theoretical challenge is to explain the origin of the relative suppression of the longitudinal response while retaining the agreement with the observed transverse response displayed by simple models.

The basic assumption that the quasielastic (e,e') reaction can be treated solely as the result of the ejection of a single nucleon from the nucleus is highly questionable. Given the size of the energy transfers to the nucleus by the scattering electron which are typical for quasielastic scattering at momentum transfers of several hundred MeV/c, it is clear that many final-state channels involving the ejection of multiple nucleons or clusters of nucleons are open. Indeed, in any treatment of the exclusive process $(e,e'N)$, which is supposed to dominate the inclusive cross section, it is necessary to allow for a substantial loss of flux to more complicated final states. This is done, for example, by using a non-Hermitean optical potential in a distorted-wave impulse approximation (DWIA) analysis of this process. Clearly, once this loss of flux is taken into account, simple integration of the exclusive process over missing energy and momentum will seriously underestimate the size of the inclusive response. The inclusive response must include contributions from all open final-state channels.

Several approaches to the final-state interactions have been proposed which revolve around a simplified treatment of the final state. The naive argument is that the final-state interaction can have no net effect on the total flux to all channels (the Coulomb sum rule) so that the details of the final-state interaction can have no appreciable effect on the inclusive quasielastic response. This attitude has resulted in calculations where the final-state interaction has simply been ignored by using the plane-wave impulse approximation (PWIA) or where the final-state interaction has been included by means of a Hermitean potential which may or may not be energy independent.[24] For simplicity, we will refer to them as shell model calculations. Unfortunately, these approaches do not adequately deal with the fact that, although the final-state interaction must conserve the total flux, it will redistribute strength as a function of energy and momentum transfer due to differences in the coupling to the available phase space. From a theoretical standpoint these shell model approaches are also unsatisfactory because the Hermitean potential, whether it be an energy-independent mean-field potential or the Hermitean part of a phenomenological optical potential, is not representative of a many-body treatment of the problem which properly includes the more complicated final-state channels. It is then difficult to determine the actual physical content of the calculations and to extend them to a more

realistic treatment of quasielastic scattering.

A physically acceptable starting point is to employ a fully realistic complex optical potential, such as those which arise from phenomenological analysis of elastic proton scattering or from associated theoretical analyses based on g-matrix or multiple scattering theories. The Green's function approach of Ref. 25 offers a satisfactory way to do this. In this approach, the relationship between forward virtual Compton scattering and inclusive electron scattering is used to construct a one-body approximation to quasielastic electron scattering. Although in Ref. 25 this approximation is motivated by arguments based in multiple scattering theory, the Green's function approach can be derived using standard projection techniques, as is done below. Consequently, the physical content of this approach can be clearly identified. It is essentially a doorway model where a single nucleon initially absorbs the virtual photon, but can couple to more complicated final channels by means of a final-state interaction. The reactive context of the non-Hermitean part of the optical potential is used to describe the many-body nature of the final-state interaction. Being well defined, this model is also extensible, allowing for the calculation of additional many-body corrections that are necessary to remove some of the dynamical inconsistencies inherent in optical model treatments of such processes. By making connection to the optical model, it is possible to constrain the final-state interaction by means of elastic nucleon-nucleus scattering, and to take advantage of the considerable body of work on the derivation and properties of microscopic optical potentials.[26–39] It should also be mentioned that a similar philosophy is the motivation for the extension of the standard RPA to the SRPA which includes multiple-nucleon knockout by calculating all particle lines in the continuum using an optical potential.[7–9] Indeed, at large momentum transfers where the effect of long-range correlations is negligible the SRPA and the optical model Green's function approach should converge provided that the dynamical input is comparable.

The objective of this paper is to provide a comprehensive study of the role of final-state interactions in inclusive quasielastic electron scattering. This study is done in the context of an optical model Green's function approach. A detailed derivation of this approach is presented in Sec. II in order to clearly identify its physical content and to clarify its limitations. The extension of this derivation to allow for complete antisymmetrization of the theory is presented in the Appendix. The incorporation of relativistic dynamics is also described in Sec. II and is done in obvious parallel to elastic proton scattering.[31,34] The computational structure of the relativistic dynamical calculation is sketched in Sec. III. Numerical results are presented in Sec. IV for both nonrelativistic and relativistic dynamics. A variety of nonrelativistic optical potentials are used, including theoretical impulse approximation (IA) potentials,[30] semitheoretical local density approximation (LDA) potentials,[26,29] and purely phenomenological potentials.[28]

Relativistic optical potentials employed span a similar range of models.[31,35] Representative results from an extensive set of calculations are presented. Using these potentials, a number of theoretical experiments are also performed to isolate the importance of various physical processes. Among the results presented are characterizations of the importance of relativistic dynamics, specific virtual pair contributions, off-shell final-state processes, and energy-dependent and non-Hermitean effects. Section V contains a summary of the results and inferences which may be drawn from our studies.

II. FORMALISM

In the one photon exchange approximation the (e,e') quasielastic differential cross section in the lab frame can be expressed in the terms of the longitudinal and transverse response functions as[40]

$$\frac{d^2\sigma}{d\Omega_{k'}d\epsilon_{k'}}=\left[\frac{d\sigma}{d\Omega_{k'}}\right]_{\text{Mott}}\left[\frac{q^4}{\mathbf{q}^4}R_L(\mathbf{q},\omega)+\left[\tan^2\frac{\theta}{2}-\frac{1}{2}\frac{q^2}{\mathbf{q}^2}\right]R_T(\mathbf{q},\omega)\right], \tag{1}$$

where the electron mass is neglected in the extreme relativistic limit assumed here. The Mott differential cross section is that obtained from the scattering of electrons from a point charge. The initial and final four-momenta of the incident electron are k and k', respectively. The initial bound-state and final asymptotic four-momenta of the ejected nucleon will be denoted by p and p', respectively. The four-momentum transfer carried by the virtual photon is denoted by q, where $q=k-k'$. The space-time coordinates and metric and Dirac algebra follow the notation of Bjorken and Drell.[41]

The longitudinal and transverse response functions are expressed in terms of the nuclear tensor, which involves the matrix elements of the virtual photon's interaction with the nuclear electromagnetic current:

$$\begin{aligned}R_L(\mathbf{q},\omega)&=W^{00}(\mathbf{q},\omega)\ ,\\ R_T(\mathbf{q},\omega)&=W^{11}(\mathbf{q},\omega)+W^{22}(\mathbf{q},\omega)\ ,\end{aligned} \tag{2}$$

where

$$W^{\mu\nu}(\mathbf{q},\omega)=\sum_i\overline{\sum_f}\langle i|\hat{J}^{\mu\dagger}(q)|f\rangle\langle f|\hat{J}^{\nu}(q)|i\rangle\times\delta(E_f-E_i-\omega)\ . \tag{3}$$

The initial target state is described by i, and f is a particular many-body final nuclear state. $\hat{J}^{\mu}(q)$ is the nuclear electromagnetic current operator, $\hat{J}^{\mu\dagger}(q)$ is the appropriate (Schrödinger or Dirac) adjoint, and $\langle f|$ is the corresponding adjoint of $|f\rangle$. Here $\overline{\sum}$ represents an average over initial states. The nuclear response tensor $W^{\mu\mu}$ can be written in terms of the virtual Compton amplitude $T^{\mu\mu}$, i.e., the elastic scattering of virtual photons from bound nucleons,

$$W^{\mu\mu}=-\frac{1}{\pi}\text{Im}T^{\mu\mu}\ , \tag{4}$$

where the virtual Compton amplitude is

$$T^{\mu\nu}=\overline{\sum_i}\langle i|\hat{J}^{\mu\dagger}(q)\hat{G}(\omega+E_i)\hat{J}^{\nu}(q)|i\rangle \ , \tag{5}$$

and $\hat{G}$ is the full many-body propagator of the complicated A-body nuclear system (where A is the atomic number of the target nucleus). To obtain the response functions an approximation method is introduced to treat the virtual Compton amplitude.

A. Reduction formalism

The nuclear response tensor as expressed in Eq. (3) or in (4) and (5) is an exceedingly complicated object which defies current computational methods. It is therefore necessary to reduce the complexity of the problem to a tractable computational form. The three basic ingredients which appear in Eq. (3)—the initial state, the final states, and the current operator which connects them—are intimately related in any theory. A given Hamiltonian specifies both the initial target wave function $|i\rangle$ and the wave functions $|\psi_f\rangle$ of all of the final nuclear states, as well as which of the latter contribute to Eq. (3) for given ω. The current operator is itself a complicated many-body operator whose exact nature depends upon the degrees of freedom described by the wave functions $|i\rangle$ and $|f\rangle$. Generally, the more the number of degrees of freedom suppressed in the wave functions, the more complicated the operator $\hat{J}^{\nu}$. This is true whether the suppressed degrees of freedom are of the fundamental meson-theoretic type or are due solely to reductions of the (A-body) nuclear many-body problem and its many degrees of freedom.

The most difficult conceptual problem in dealing with Eq. (3) is determining a realistic procedure for handling the continuum of final states with their complex many-nucleon knockout character. Simplifications of $\hat{J}^{\nu}$ and $|i\rangle$ introduced to facilitate analysis of the final-state continuum in this subsection will be addressed in their own right in Sec. II B. Suppose the current operator $\hat{J}^{\nu}$ is so simple that it directly couples the initial target state $|i\rangle$ only to one-nucleon knockout states, that is, only to the space spanned by a plane-wave nucleon and an (A-1)-body residual nuclear eigenstate. Denoting these channels by α_i, the associated eigenstates of the (A-1)-body Hamiltonian H_{α_i} by $|\phi_{\alpha_i}\rangle$, defining projectors onto the subspaces in the standard way

$$P_{\alpha_i}=|\phi_{\alpha_i}\rangle\langle\phi_{\alpha_i}| \ , \tag{6a}$$

and defining the projector onto the full one-nucleon knockout space

$$\Pi=\sum_{\alpha_i}P_{\alpha_i} \ , \tag{6b}$$

Eq. (5) becomes

$$T^{\nu\nu}=\overline{\sum_i}\langle i|\hat{J}^{\nu\dagger}(q)\Pi\hat{G}\Pi\hat{J}^{\nu}(q)|i\rangle \ . \tag{7}$$

The special case where $|i\rangle$ is just a single Slater determinant is useful to keep in mind as a simple, concrete example. In that case the α_i just refer to the set of (A-1)-body residual nuclear states ($|\phi_{\alpha_i}\rangle$) that can be formed from the target by removing one nucleon. Except for the azimuthal degeneracies, these are just the few occupied subshells in number. A further approximation,

$$\Pi\hat{G}\Pi\approx\sum_{\alpha_i}P_{\alpha_i}\hat{G}P_{\alpha_i} \ , \tag{8}$$

is introduced so that Eq. (7) becomes

$$T^{\nu\nu}=\overline{\sum_i}\sum_{\alpha_i}\langle i|\hat{J}^{\nu\dagger}(q)P_{\alpha_i}\hat{G}P_{\alpha_i}\hat{J}^{\nu}(q)|i\rangle \ . \tag{9}$$

Equation (8) is discussed in more detail in the next subsection. In writing Eqs. (7)–(9) the Pauli requirement that only properly antisymmetrized states contribute to the spectral form of $\hat{G}$ (see Appendix A) has not been made explicit. The reason for this is that in proceeding further it is desirable to work overtly with a distinguishable ejectile so as not to needlessly obscure essential points. Although there are some interesting theoretical points associated with the fully antisymmetrized treatment, which is presented in Appendix A, all of our main results, namely Eqs. (16)–(19), remain unchanged. It is now noted that

$$P_{\alpha_i}\hat{G}P_{\alpha_i}=G^{\alpha_i}_{\rm opt} \ , \tag{10}$$

where $G^{\alpha_i}_{\rm opt}$ is the α_i-channel one-body optical model Green's function as it is usually defined,[27,36–38] with optical potential $V^{\alpha_i}_{\rm opt}$. This result follows immediately from the combination of the resolvent identity

$$\hat{G}=G_{\alpha_i}+G_{\alpha_i}V^{\alpha_i}\hat{G} \tag{11}$$

(right and left projected by P_{α_i}) and the definition of the optical potential U_{α_i} in terms of the α_i-channel elastic T matrix T^{α_i}:

$$T^{\alpha_i}=U^{\alpha_i}+U^{\alpha_i}P_{\alpha_i}G_{\alpha_i}T^{\alpha_i} \ , \tag{12}$$

where

$$T^{\alpha_i}=V^{\alpha_i}\hat{G}G^{-1}_{\alpha_i} \ , \tag{13}$$

$$V^{\alpha_i}_{\rm opt}=P_{\alpha_i}U^{\alpha_i}P_{\alpha_i} \ , \tag{14}$$

and $G_{\alpha_i}=(E-H_{\alpha_i})^{-1}$ is the α_i-channel free propagator (for the noninteracting nucleon/residual nuclear system). As a final approximation we take

$$V^{\alpha_i}_{\rm opt}\approx V_{\rm opt} \ , \tag{15}$$

where $V_{\rm opt}$ is a specific one-body optical potential, for example, the one associated with the initial target nucleus. Equation (9) now takes the form

$$W^{\nu\nu}\cong-\frac{1}{\pi}{\rm Im}\left\{\overline{\sum_i}\sum_{\alpha_i}\langle i|\hat{J}^{\nu\dagger}(q)P_{\alpha_i}G_{\rm opt}P_{\alpha_i}\hat{J}^{\nu}(q)|i\rangle\right\} \ , \tag{16a}$$

$$\cong-\frac{1}{\pi}{\rm Im}\left\{\overline{\sum_i}\sum_{\alpha_i}\langle i|\hat{J}^{\nu\dagger}(q)|\phi_{\alpha_i}\rangle G_{\rm opt}\langle\phi_{\alpha_i}|\hat{J}^{\nu}(q)|i\rangle\right\} \ . \tag{16b}$$

Finally, in momentum-space it is convenient to employ a nonspectral form for the optical model Green's function $G_{\rm opt}$ and rewrite Eq. (16b) in the form

$$W^{\nu\nu} \cong -\frac{1}{\pi}\mathrm{Im}\left\{\overline{\sum_i}\sum_{\alpha_i}\langle i|\hat{J}^{\nu\dagger}(q)|\phi_{\alpha_i}\rangle(g_0+g_0T_{\rm opt}g_0)\langle\phi_{\alpha_i}|\hat{J}^{\nu}(q)|i\rangle\right\}, \tag{16c}$$

where g_0 is the free one-body Green's function and $T_{\rm opt}$ is the optical model T matrix. Exactly the same equations, (16), are obtained from the fully antisymmetrized development (see Appendix A). Equation (16c) is of the form actually employed in our numerical work as is discussed in Sec. III. With the addition of not-too-complicated models for $\hat{J}^{\nu}(q)$, and for the ground and excited wave functions $|i\rangle$ and $|\phi_{\alpha_i}\rangle$, Eq. (16) is pragmatically calculable, requiring as further input only the off-shell T matrix $T_{\rm opt}$. Better yet, Eqs. (16) reduce the sum over the complicated many-body final states to a form that exhibits great conceptual clarity. Using Eq. (10) and the spectral decomposition of the full Green's function, Eq. (16) can be rewritten as

$$W^{\nu\nu} \cong \overline{\sum_i}\sum_{\alpha_i}\langle i|\hat{J}^{\nu\dagger}(q)P_{\alpha_i}\left[\sum_f|\psi_f\rangle\delta(\omega+E_i-E_f)\langle\psi_f|\right]P_{\alpha_i}\hat{J}^{\nu}(q)|i\rangle, \tag{17a}$$

manifesting the treatment of the $|\psi_f\rangle$. Let $|\psi_F\rangle$ denote a final state of arbitrary complexity, say for example it is a state which asymptotically corresponds to five-nucleon knockout. In the vicinity of the residual nucleus, $|\psi_F\rangle$ consists of a superposition of many configurations of all asymptotic characters, including a Π-space component, $\sum_{\alpha_i}\langle\phi_{\alpha_i}|\psi_F\rangle|\phi_{\alpha_i}\rangle$. It is this latter part of $|\psi_F\rangle$ which in Eq. (17) couples directly to the ground state through the current operator. More generally,

$$W^{\nu\nu} \cong \overline{\sum_i}\sum_{\alpha_i}\langle i|\hat{J}^{\nu\dagger}(q)|\phi_{\alpha_i}\rangle\left[\sum_f\langle\phi_{\alpha_i}|\psi_f\rangle\delta(\omega+E_i-E_f)\langle\psi_f|\phi_{\alpha_i}\rangle\right]\langle\phi_{\alpha_i}|\hat{J}^{\nu}(q)|i\rangle . \tag{17b}$$

Thus, the set of A-body states which comprise the P_{α_i} serve as doorways to channels of arbitrary complexity. Such channels are then incorporated, albeit approximately, in the formalism of Eq. (16).[42] Equation (16c), which was first exploited in Ref. 25, forms the basis for the analysis in this paper. It goes far beyond simple plane-wave or real potential models in providing a clear conceptual treatment of complex many-body reaction channels. It will become clear that it also provides for a straightforward set of immediate correction terms.

To see exactly how Eq. (16) extends the analysis of inclusive quasielastic (e,e') beyond simple integrations over the one-nucleon knockout space, it is noted that the unitarity relation satisfied by a generic one-body Green's function, g, with (possibly) non-Hermitean optical potential $V_{\rm opt}$ is ($\Delta A \equiv A - A^{\dagger}$)

$$\Delta g = (1+V_{\rm opt}g)^{\dagger}\Delta g_0(1+V_{\rm opt}g)+g^{\dagger}\Delta V_{\rm opt}g \tag{18a}$$

$$= -2\pi i(1+V_{\rm opt}g)^{\dagger}\delta(E_i+\omega-h_0)\times(1+V_{\rm opt}g)+g^{\dagger}\Delta V_{\rm opt}g , \tag{18b}$$

where h_0 is the free one-body Hamiltonian and where in writing Eq. (18b) the parametric energy, z of Eq. (18a) is taken to be $z=E_i+\omega$. The operator $(1+gV_{\rm opt})$ is just the familiar Möller operator which, when operating on a plane-wave state of the same energy, produces the corresponding (outgoing scattered wave) distorted wave. Thus, with $|\chi_{\mathbf{k}}\rangle$ denoting a distorted wave of asymptotic momentum $\mathbf{k}$ and incoming scattered wave boundary conditions,[43]

$$\Delta g = -2\pi i\int d^3k|\chi_{\mathbf{k}}\rangle\delta(E_i+\omega-E_k)\langle\chi_{\mathbf{k}}|+g^{\dagger}\Delta V_{\rm opt}g . \tag{18c}$$

Comparing Eq. (18) with Eq. (16) for inclusive quasielastic scattering, a plane-wave integration within the one-body knockout space corresponds to keeping just the Δg_0 part of the first term of Eq. (18), while using only the real part of $V_{\rm opt}$ in such a calculation corresponds to dropping the last term of Eq. (18) entirely and using only $\mathrm{Re}(V_{\rm opt})$ in the first term of Eq. (18). The combination of Eq. (16) and Eq. (18) thus makes evident the additional physics obtained in Eq. (16), as opposed to calculations that consider only the one-body knockout space of $(e,e'N)$. Similarly, Eq. (18) makes clear the crucial correction contained in Eq. (16), specifically the second term of Eq. (18), which goes far beyond a simple integration over the one-body knockout space in the context of a non-Hermitean optical model.

Finally, because Eq. (13) for T^{α_i} is Hermitean analytic [$T^{\alpha_i}(z^{\dagger})=T^{\alpha_i}(z)^{\dagger}$, where z is the (complex) parametric energy] and because the structure of Eq. (12) passes this property on to U^{α_i}, $V_{\rm opt}(z)$ is Hermitean analytic. Thus the one-body optical potential $V_{\rm opt}$ satisfies the once-subtracted dispersion relation (E real)

$$\mathrm{Re}V_{\rm opt}(E)=\mathrm{Re}V_{\rm opt}(0)+\frac{E}{\pi}\mathcal{P}\int\frac{\mathrm{Im}V_{\rm opt}(E')}{E'(E'-E)}dE' , \tag{19}$$

where it has been assumed that $V_{\rm opt}(z)$ falls off fast enough as $|z|\to\infty$ and that there are no singularities of $V_{\rm opt}(z)$ other than the cut along the positive real axis. The significance of Eq. (19) in regard to practical calculations and the Coulomb sum rule is discussed in the following subsection.

B. Approximations, limitations, and corrections

Although the approach of Ref. 25 provides an advantageous basis on which to construct a detailed treatment of

the inclusive quasielastic (e,e') reaction, several demanding assumptions have already been made in obtaining Eqs. (16). These assumptions need to be more clearly stated in the form of approximations and, in addition, several more approximations are required to reduce the problem to the practical calculation described in detail in Sec. III. Here, the approximation scheme, the limitations of the approach, and the leading corrections to it are discussed.

This discussion clarifies not only the physical content of the calculations which we perform but also puts them into perspective relative to other existing calculations and indicates necessary improvements for future work. In order to arrive at (16) it has been necessary to make several assumptions or approximations. These are (1) the current operator only couples the target ground state to those of the scattering states which lie in the one-body knockout space, (2) partial decoupling of the one-body knockout channels [Eq. (8)], and (3) a common optical potential for all channels α_i [Eq. (15)]. Additional approximations are also necessary in order to produce a practical calculation, these are (4) practical approximations for the formally exact operator $V_{\rm opt}$, (5) full antisymmetrization and analytic properties versus practical approximations to $V_{\rm opt}$, and (6) practical approximations to the true many-body bound states $|i\rangle$ and $|\phi_{\alpha_i}\rangle$. Consider each of these six items in turn.

(1) This assumption is the key ingredient of the whole approach. Starting from an elementary current operator in a theory without (acknowledged) suppressed degrees of freedom, one begins with a simple form consisting of a contributing current from each elementary electromagnetically coupled particle. Upon suppressing some of these degrees of freedom, i.e., the explicit appearance of certain final states in the wave functions, a more complicated effective current operator results. In general, this effective current operator will have two- and many-body components. The standard example of this is, of course, the suppression of mesonic and virtual pair degrees of freedom and the resultant effective meson exchange current operators. Similarly, the suppression of purely many-fermion (A-body) degrees of freedom in truncated bound state, one-body optical model, RPA, or coupled-channel theories also implies more complicated effective current operators. The degrees of freedom suppressed in the wave functions are embedded in the effective current operator.

In this paper, all results are calculated on the basis of the usual form of the Dirac free-nucleon current operator. Thus, the free nonrelativistic current and some pair current effects are included. The use of such a free current operator is justified on the basis of simplicity and as a starting point only. It breaks gauge invariance, the current is not conserved, and it is not physically consistent with the wave functions employed. Estimates indicate that ambiguities introduced from this source are at least non-negligible.[44] A firmer basis is needed and corrections must be carefully considered.

There already exists a large literature concerning meson exchange current corrections to approaches such as that employed here.[45] For longitudinal response functions these are usually small, due to Siegert's theorem.[46] For the transverse currents these corrections also tend to be small in the region where the one-body current maintains appreciable strength, but can be appreciable in a relative sense once the one-body contribution has fallen off, for example at large q.[45] At any rate, the technology for treating such corrections is well developed and can be easily included in the present context. This should prove physically interesting in appropriate regions of four-momentum transfer such as in the dip region between the transverse response and the delta-resonance peak. Effective current operator components that result from truncations of many-body scattering and bound-state wave functions are not so well documented. Two-body currents resulting from truncated nuclear bound-state wave functions are readily accessible, while the analysis of currents implied by optical model truncations of the continuum scattering states is not so readily conceived.

With this background, assumption (1) can be characterized as follows. For the one-body part of the current operator it is a very reasonable approximation. For two-body and higher-order currents this approximation is not likely to be so reliable, since the current operator can then couple directly to N-nucleon knockout, where $N \geq 2$, even in the case of a single Slater determinant for the target ground state. Thus, the one-body free current operator and one-body correction terms to it should reasonably be expected to be well-treated within the context of Eq. (16), at least so long as the $|\phi_{\alpha_i}\rangle$ are well described as a superposition of one-hole states built upon the target ground state (so that the one-hole strength remains concentrated in Π). Bound-state many-body corrections to the effective current operator can be investigated more directly by simply employing more sophisticated bound-state wave functions. This should not be affected by assumption (1) except to the extent that the assumed concentration of the one-hole strength in Π is further compromised. Finally, two- and many-body current operator corrections from the optical model truncation are the most problematic elements. To the extent that they turn out to be small, they may be subsumed into the characterization of the exchange currents. However, because of their intrinsic many-body character, they may be more difficult to handle. This issue needs further attention.

(2) Equation (8) is not required to arrive at a doorway model of the general type of Eqs. (16), but is only needed to reduce the problem from coupled channel to one-body optical model form. Equation (8) effectively requires only that there be no interference among different doorway channels. This will be a good approximation so long as no "important" final state $|f\rangle$ has appreciable components of more than one doorway state.

Consider first the case of the one-body part of the current operator. From assumption (1), it is assumed that photoejection starts the system in a particular state in the doorway space. If this state asymptotically ends up in a one-body knockout final state, it is very likely that this will be the same particular doorway state, unless there are strongly coupled collective states. Because the states $|\phi_{\alpha_i}\rangle$ are eigenstates of the Hamiltonian H_{α_i}, they

both are orthogonal and specify the final asymptotic configuration of the system when it ends up in the Π space. Thus, under the stated condition, it is unlikely that such a final state will have an appreciable doorway component other than that which it ends up in. Corrections to this approximation are of order $(1/A)$ and are of the type typically neglected in first order in optical model theories.[31,38,39] Note that this approximation does *not* entail a simplified nuclear structure description, but only requires that multiple elastic scattering by the ejectile dominate net inelastic transitions within the Π space.

For more complicated final states, however, this approximation is not likely to do as well. Consider, for example, two-body knockout processes in our single Slater determinant example. In this case the final state $|f\rangle$ may be reached by photoejection to form a particular α_i-channel hole state, followed by nucleon knockout by the photoejectile. Obviously, the resultant two-hole state can be reached in two ways, starting with two different α_i channels. It is then evident that interference effects among the α_i channels will generally be important, since $|f\rangle$ will now have appreciable components of more than one of the $|\phi_{\alpha_i}\rangle$ doorway states. It is of course not surprising that one-body optical model analyses should display some defects in their ability to describe two-body and higher knockout. Thus, for treating contributions from higher-order knockout, a coupled-channel optical model treatment may provide for a more reliable analysis. For the effective two-body current the foregoing discussion remains relevant, except that physically one now has the potential for direct photoejection of two nucleons. This adds another interfering mechanism which can feed two-nucleon knockout and would seem to make α_i-channel interference effects even more cogent for analyzing two-body knockout events. This is somewhat academic, however, unless one relaxes the assumption (1) and extends the analysis beyond Eq. (7).

It is clear that at least in some cases, at lower energies or momentum transfers and more generally for exploratory purposes, it will be desirable to avoid Eq. (8) and instead employ an overall optical model analysis in conjunction with an explicit coupled-channel description of the Π space. Of course, a simple Hermitean coupled-channel approach within the Π space is not physically sufficient in and of itself. Non-Hermitean optical potentials are still required to treat the important coupling to suppressed channels. It is then clear that such an extension must contain all of the physical effects of Eq. (16), and more. Thus, the importance of a realistic treatment of final-state dynamics which follows from our numerical results can only be further enhanced.

(3) The use of a common optical potential for all of the α_i channels is perhaps the best justified of the major approximations. In the absence of strongly coupled collective states, and as long as Π concentrates the one-hole strength, the various $|\phi_{\alpha_i}\rangle$ and $|i\rangle$ differ from each other by effects of order $(1/A)$. In the example of a single Slater determinant, the residual nuclear wave functions $|\phi_{\alpha_i}\rangle$ differ from the initial target wave functions $|i\rangle$ by the absence of a single filled nucleon state and from each other by the single-particle state occupied by one nucleon. Many effects of order $(1/A)$ are characteristically neglected in optical model and distorted-wave analyses, both formally and practically. Corrections to such approximations typically show little effect on computed results, except in cases where the first-order optical potential is specially limited in effect.

(4) The formally exact operator $V_{\rm opt}$ is a very complicated operator with a complex analytic structure reflecting the numerous many-body energy-dependent channel effects subsumed within U^{α_i}. In addition, all of the complexity associated with the many-body bound states $|\phi_{\alpha_i}\rangle$, through which the P_{α_i} are defined, are present as well. Dealing directly with the full operator $V_{\rm opt}$ is essentially as complicated as solving the original many-body problem itself. Thus it is hardly surprising that this operator must be drastically approximated in computational applications. Consequently, much of the formal content of $V_{\rm opt}$ employed in the developments of Sec. II A is either lost or only crudely represented. In fact, except in certain circumstances, to say that this operator is approximated is really overly optimistic since the actual approximations involved are not known. A more realistic view is that the operator is simply truncated in a more or less phenomenological manner.

At low energies where individual many-body channels rapidly open as the energy increases and thresholds are reached, the formal optical potential varies rapidly with energy and has a complicated structure.[27] In this regime no completely satisfactory formal development exists and it is probable that current methods, including phenomenology, fail to do justice to the problem. However, as the energy increases to the intermediate energy regime, theoretical treatments become more realistic, especially multiple scattering methods, and approximations are under better control. This is typified by the great similarity between phenomenological and theoretical optical potentials and their predicted on-shell scattering amplitudes. Thus it is in this regime that the treatment of final-state interactions is likely to be most adequate.

In this paper, nonrelativistic optical potentials from phenomenology,[28] local density approximation,[26,29] and microscopic multiple scattering theory[30] are employed. Relativistic optical potentials are generalizations which are constructed more or less in parallel to the corresponding nonrelativistic approach.[31] At low nucleon energies (≤ 100 MeV), and as a realistically energy-dependent operator, it is probable that only purely phenomenological optical potentials are at all reasonable. At intermediate energies (≥ 100 MeV) phenomenological optical potentials of course still most accurately describe the on-shell nucleon-nucleus T matrix but the multiple scattering theory is best understood conceptually and as a source of off-shell behavior. Here, the convergence of theory and phenomenology indicates that it is not unreasonable to hope that the various optical models are representative of the nature of the true $V_{\rm opt}$ and that their differences reasonably gauge our uncertainty in this regard.

(5) As noted in assumption (4) much of the analytic

structure of $V_{\rm opt}$ is lost when drastic approximations necessitated by current methods are made. It is thus necessary to consider whether there are specific constraints which can and need to be imposed on approximate theoretical or phenomenological optical potentials which are to be employed in inclusive quasielastic electron scattering. The fragile nature of unitarity and dispersion relations, especially in the fully antisymmetrized formalism, is discussed in Appendix A. Of course, detailed unitarity and dispersion properties of $V_{\rm opt}$ are always violated in approximation schemes. Our concern here is that global unitary and dispersion properties of $V_{\rm opt}$ may be unnecessarily violated as well and that this may unduly prejudice (e,e') quasielastic predictions. For example, in Ref. 25 it was observed that, in a particular model, theoretically predicted quasielastic strength systematically overshot experimental data. This problem was found to be correlated with apparent Coulomb sum rule violations by the calculation of the order of 5–10 %. It was then observed that both problems were apparently rectified by imposing the dispersion relation (19). Reference 25 then remarks that "It is interesting to note that quasielastic electron scattering is apparently sensitive to the analytic structure of the optical potential."

However, it is not entirely clear exactly what the essential physics associated with the imposition of relation (19) actually is. Obviously Eq. (19) can be used to prevent accidental and unphysical singularities from appearing in the analytic structure of approximate $V_{\rm opt}$ off the positive real energy axis. Equally as obvious, Eq. (19) is too strong. It does not follow from Eq. (12) and Eq. (14). For example, Eq. (19) assumes that there are no discrete pole singularities in $V_{\rm opt}$ along the positive real axis and thus forbids associated resonance structure in the physical scattering amplitude.[32] In reality this may be physically important at low energies and it is certainly relevant to Coulomb sum rule saturation. Moreover, it is not clear from what significant underlying physical source the excluded singularity structure is derived. Thus, especially in the case of theoretically derived optical potentials, use of Eq. (19) remains problematical. It is not clear, for example, that Eq. (19) should be used in energy-dependent analyses for joining theoretical models of $V_{\rm opt}$ to phenomenology in regions where the former breaks down, or whether improved energy-dependent phenomenology is to be preferred. No clear constraint of the type of relation (19) is yet apparent.

One constraint which is apparent is the one-body completeness relation and its essential role in preserving the nonrelativistic Coulomb sum rule. Obviously, nonrelativistic analyses which appreciably violate this relation cannot be seriously compared to experiment. One of the advantages of the Green's function approach in Eqs. (16) is its automatic faithfulness to the completeness relation. In fact, for non-Hermitean optical potentials, this is the essential function of the last term of Eq. (18). In the analysis of Eqs. (16) a nonspectral form of the optical model Green's functions is employed, wherein Eq. (16c) is treated by integrating over the scattering amplitude $T_{\rm opt}$ (see Sec. III). It is then important that Eqs. (16) guarantee consistency with the completeness relation. For example, it follows that the calculation incorporates any bound states in the continuum[47] that may be present. Such normalizable states can arise, in the presence of non-Hermitean potentials, as complex eigenvalues. These states are (bi)orthogonal to the scattering eigenfunctions, which have real eigenvalues. Thus the continuum bound states are not of the character of resonances, and do not lie in the space spanned by the scattering eigenfunctions. In the event that such states exist for a given optical potential they must be included in the completeness relation in order to span the space. This is done automatically in the formalism of Eq. (16c), which includes these wave functions as well as those with scattering boundary conditions. Thus, it is unnecessary to explicitly check for the existence of such solutions. On the other hand, such solutions are unphysical in the present case because the optical potential is supposed to reproduce

$$T_{\rm opt}=P_{\alpha_i}T^{\alpha_i}P_{\alpha_i}\ , \tag{20}$$

where T^{α_i} is the true many-body scattering amplitude, which encompasses no such continuum bound states. Thus, for the present case, realistic optical potentials can reasonably be supposed to have no such states and optical potentials that do produce continuum bound states may best be regarded as being unsuitable.

(6) The true many-body bound states $|i\rangle$ and $|\phi_{\alpha_i}\rangle$ must be approximated in practical calculations. This problem has been alluded to in the preceding discussion of approximations to $V_{\rm opt}$. In practice virtually all calculational methods are based on the simple independent particle shell model. Improvements to the wave functions above the simple shell model are typically represented by particle-hole excitations of a closed-shell basis. In this context the II space represents all possible hole states in the A-body ground state and assumption (1) is equivalent to the assumption that the current operator is a one-body operator. Introducing short-range correlations into the description of the bound states results in two-particle–two-hole excitations, which in combination with even a one-body current operator can result in two particles in the continuum and two holes in the residual system. Therefore, even if only the one-body current operator is used, consistent with assumption (1), the introduction of short-range correlations makes it possible to couple directly into the space complimentary to the II space. As a practical matter, part of these contributions may be subsumed into an effective current operator in the optical model doorway model, but others which continue to propagate in the complimentary space are effectively excluded from the optical model treatment.

Although the discussion is framed in the context of the optical model treatment of quasielastic scattering, it should be clear that calculations may be carried out using other schemes. Whatever the approach, unitarity and electromagnetic current conservation require that all final-state channels included in a calculation, either explicitly or implicitly, must be treated consistently. For example the optical model calculations, which we present below, contain two-nucleon knockout channels implicitly in the optical potential, but do not properly include con-

tributions to the same channel which arise from short-range correlations. As a result these calculations do not conserve current. Estimates indicate that ambiguities introduced from this source are non-negligible.[44]

With the discussion above, it is possible to make comparisons between the physical content of various existing calculations and the optical model results which we present below. The RPA calculations are designed to improve the description of the wave function and to treat the coupling of the P_{α_i} channels at a level where all asymptotic excitations are within the Π space. As discussed in (2) these effects are expected to be large at low momentum transfers where it is possible to excite long-range collective states in the residual system. Indeed, these calculations show that RPA corrections are important in the longitudinal response at low momentum transfers but become negligible by about 400–500 MeV/c.[7]

The second RPA (SRPA) approximation is a hybrid of the RPA and optical model approaches. Optical potentials are used for particle lines in the continuum to account for loss of flux to multiple particle-hole channels and a hole-line optical potential is introduced to improve the description of the evolution of the $|\phi_{\alpha_i}\rangle$ states. These calculations also indicate that the importance of RPA corrections diminish with increasing momentum transfer as do the hole-line corrections. At momentum transfers greater than 500 MeV/c the results are consistent with the optical model approach, where the dressings on the particle line dominate.[9]

Meson exchange current effects have been calculated within the context of simple models. Calculations of 1p-1h (Ref. 48) and 2p-2h (Ref. 49) excitations resulting from meson exchange currents have been carried out in mean field calculations. The 1p-1h contributions result in modifications to the transverse response of 10–20%, while the 2p-2h can produce substantial contributions to the transverse response above the quasielastic peak, as was the case in earlier Fermi gas calculations.[50]

To date, the only calculations of the effects of short-range correlations on quasielastic scattering from many-body systems have been carried out in nuclear matter.[51,52] Reference 51 uses the orthogonalized correlated basis method for nuclear matter in an expansion consistent to the 2p-2h level relative to this basis. Only the longitudinal response is calculated, but significant and interesting effects arise from the introduction of the 2p-2h states. Reference 52 is a nuclear matter Brueckner theory calculation consistent to the two-hole level in the hole-line expansion. Unfortunately, the calculation uses a factorization approach to study y scaling of the spectral function. Therefore, the effects resulting from differences between longitudinal and transverse current operators or exchange currents are not included and detailed information concerning the effect of the consistent expansion over the complete quasielastic region was not presented.

It is clearly desirable from considerations of both physics and aesthetics to have finite nucleus calculations which are completely consistent to the 2p-2h level. However, the necessity of dealing with two-body exchange currents makes this an extremely difficult task. Before undertaking such an effort it is useful to determine whether or not the inclusion of such final states appreciably affects the quasielastic response functions. The optical model approach is well suited to this purpose and as will be seen below indicates that the inclusion of such states significantly modifies the quasielastic response even at relatively large momentum transfers.

Finally the most important role of the nuclear structure lies perhaps in its determining the validity of the key assumption of our whole treatment, namely, assumption (1). Only if the one-hole strength is concentrated in the Π space is this assumption justified. Moreover, the degree to which this assumption is broken in more sophisticated nuclear structure models can determine an overall multiplicative factor in the calculated current matrix elements of the one-body current, as well as the nature of correction terms which must be considered in this regard.

Although the various approximations above are obviously both extensive and demanding, it is also clear that Eq. (16) forms a very firm basis for a realistic theoretical development. It is conceptually clear in formal content and approximations, while going well beyond previous approaches. The main sequence of approximations seems very well justified in a "first-order" sense. Many corrections and their characters are well circumscribed. Areas where further work is needed are clearly indicated.

C. Relativistic extension

The preceding subsections contain a full formal development for inclusive quasielastic electron scattering within the context of the nonrelativistic Schrödinger equation. There is no corresponding development for the relativistic dynamical extension. Although relativistic field theory provides a complete formal development in principle, it has not yet yielded a sound development at the level of practical feasibility. This is mainly because of the complexity of the diagrammatics and the associated renormalization program, which so far has made impossible the clear determination of leading relativistic corrections, even for few fermion systems. Unambiguous extraction of such corrections from a field theoretic description of an interacting many-body system is beyond the realm of current methods.

Given this circumstance, one must be satisfied with gauging the implications of "leading" relativistic effects of a more or less intuitive nature, without the benefit of a completely consistent means for doing so. In this paper we focus on possible physical effects which may result from a Dirac dynamical description of the bound and ejected nucleons. Basically, this entails a single-particle description of the (bound, ejected) nucleon in which the one-body Dirac equation in the presence of a (Hermitean, complex) potential is obeyed. The Dirac bound-state wave functions employed are those of Ref. 53, while the optical model description of the relativistic final-state interaction of the ejectile is taken from Refs. 31, 35, and 53, as described in more detail in Sec. III. The final ingredient needed to specify the relativistic extension of Eq. (16c) employed in this paper is a relativistic current operator. The usual form of the free Dirac electromag-

netic current operator is used without any nonrelativistic reductions.

This relativistic extension of the formalism of the preceding subsections has at least two main advantages. First, the extension is done in obvious parallel to Dirac dynamical treatments of elastic proton scattering, the physical process which has so far been the primary domain for such relativistic extensions. Second, the momentum-space approach employed in conjunction with the relativistic extension enables one to, among other things, adopt a closely parallel nonrelativistic limit. One does this[44] by simply imposing on the relativistic wave functions the requirement that the lower components of the Dirac spinors be fixed at the appropriate free-particle value for each value of the momentum. This effectively reduces the problem from four- to two-component spinors, i.e., from Dirac-to-Pauli spin space. One can thus break the relativistic momentum-space wave function into two parts, a "nonrelativistic Pauli wave function" multiplied by the matrix which converts the Pauli spinor into the corresponding free Dirac spinor (see, e.g., Ref. 44 for more detail). This is in the same spirit, as nonrelativistic operators are often defined from matrix elements of their relativistic counterparts, namely, by lumping these Pauli-to-Dirac conversion matrices together with the relativistic operator to put the matrix element into a nonrelativistic form. For example in the present case the Pauli-to-Dirac conversion matrices and the Dirac current operator can be combined, thus formally rewriting the relativistic current matrix element in terms of nonrelativistic (Pauli) wave functions and an associated nonrelativistic current operator. This is in effect what the definition of our nonrelativistic limit does. It is also noted that the reduction from four to two component spinors described above corresponds to eliminating any negative-energy (i.e., antiparticle and pair) degrees of freedom in the wave function; that is, this reduction confines the wave functions to the positive-energy particle sector of the Dirac-Hilbert space.

III. CALCULATIONS

In this section the methods used in the practical implementation of the reduced formalism, as developed in the preceding section, are presented in detail. Actual numerical results are discussed in the following section. Because the nonrelativistic case is a straightforward simplification of the relativistic one, the computational structure used for the relativistic calculations is the one explicitly treated.

To calculate the nuclear response, the virtual Compton amplitude is expressed using Eqs. (5) and (16b) as

$$T^{\mu\nu}=\overline{\sum_i}\sum_{\alpha_i}\langle i|\hat{J}^{\mu\dagger}|\phi_{\alpha_i}\rangle\hat{G}_{\rm opt}(\omega+E_i)\langle\phi_{\alpha_i}|\hat{J}^{\nu}|i\rangle\ . \tag{21}$$

In the numerical evaluation of Eq. (21) the usual form of the free Dirac current operator is employed and a variety of optical potentials are investigated as sources for $\hat{G}_{\rm opt}(\omega+E_i)$. Since the focus is on dynamics in this paper, a simple Slater determinant of one-body nuclear states is employed to represent the target ground state wave function $|i\rangle$. Corrections due to more sophisticated nuclear structure models are not expected to be crucial in the momentum transfer region of interest in this study. Similarly, the one-body knockout states $|\phi_{\alpha_i}\rangle$ are taken to differ from $|i\rangle$ only in the absence of the ejected nucleon so that differences between the target and residual nuclear Hamiltonians are neglected. With these approximations, the one-body nature of $\hat{J}^{\mu}$ is sufficient to reduce Eq. (21) to a one-body matrix element, provided one also ignores nonorthogonality terms which arise from the nonzero overlap of distorted waves and single-particle bound-state wave functions. Thus, Eq. (21) becomes

$$T^{\mu\nu}=\sum_i\langle\overline{i_{(1)}}|\hat{J}^{\mu\dagger}_{(1)}\hat{G}_{\rm opt}(\omega+E_i)\hat{J}^{\nu}_{(1)}|i_{(1)}\rangle\ . \tag{22}$$

where the sum is over the nuclear single-particle states $|i_{(1)}\rangle$ which are occupied in the target, the subscript (1) is used to emphasize the one-body nature of the quantities which appear in Eq. (22), the Dirac adjoint state has been made explicit, and the $\dagger$ denotes the Dirac adjoint for the remainder of this section.

This expression for the virtual Compton amplitude is given in momentum space by

$$T^{\mu\nu}=\sum_i\int\frac{d^3l\,d^3\mathbf{p}\,d^3\mathbf{p}'\,d^3l'}{(2\pi)^{12}}\langle\overline{i_{(1)}}|l\rangle\langle l|\hat{J}^{\mu\dagger}_{(1)}|\mathbf{p}\rangle\langle\mathbf{p}|\hat{G}_{\rm opt}(\omega+E_i)|\mathbf{p}'\rangle\langle\mathbf{p}'|\hat{J}^{\nu}_{(1)}|l'\rangle\langle l'|i_{(1)}\rangle\ , \tag{23}$$

where the matrix elements are

$$\begin{aligned}
&\langle l|\hat{J}^{\mu\dagger}_{(1)}|\mathbf{p}\rangle=J^{\mu}(-q)(2\pi)^3\delta^{(3)}(l-\mathbf{p}+\mathbf{q})\ ,\\
&\langle\mathbf{p}'|\hat{J}^{\nu}_{(1)}|l'\rangle=J^{\nu}(q)(2\pi)^3\delta^{(3)}(l'-\mathbf{p}'+\mathbf{q})\ ,\\
&\langle\mathbf{p}|\hat{G}_{\rm opt}(\omega+E_i)|\mathbf{p}'\rangle=(2\pi)^3G_{\rm opt}(\mathbf{p},\mathbf{p}';E),\quad E=\omega+E_i\ .
\end{aligned} \tag{24}$$

In Eq. (24) the bar indicates a Dirac conjugate, $\langle\bar{l}|l\rangle=\langle l|i\rangle^{\dagger}\gamma_0$ and $G_{\rm opt}(p,p';E)$ is the full one-body optical model Green's function. The virtual Compton amplitude is thus

$$T^{\mu\nu}=\sum_i\int\frac{d^3\mathbf{p}\,d^3p'}{(2\pi)^3}\langle\bar{i}|\mathbf{p}-\mathbf{q}\rangle j^{\mu}(-q)G_{\rm opt}(p,p';E)J^{\nu}(q)\langle\mathbf{p}'-\mathbf{q}|i\rangle\ . \tag{25}$$

The optical model propagator is then written as

$$G_{\rm opt}(p,p';E)=G_0(p)\delta^{(3)}(\mathbf{p}-\mathbf{p}')+G_0(p)T_{\rm opt}(p,p';E)G_0(p')\ , \tag{26}$$

where $G_0(p)$ is the free Dirac propagator and $T_{\rm opt}(p,p';E)$ is the fully off-shell Dirac optical model nucleon-nucleus T matrix. Combining Eqs. (25) and (26) yields

$$T^{\mu\nu}=\sum_i\int\frac{d^3\mathbf{p}}{(2\pi)^3}\langle\bar{i}|\mathbf{p}-\mathbf{q}\rangle J^\mu(-q)G_0(p)J^\nu(q)\langle\mathbf{p}-\mathbf{q}|i\rangle$$
$$+\sum_i\int\frac{d^3\mathbf{p}\,d^3\mathbf{p}'}{(2\pi)^3}\langle\bar{i}|\mathbf{p}-\mathbf{q}\rangle J^\mu(-q)G_0(p)T_{\rm opt}(p,p';E)G_0(p')J^\nu(q)\langle\mathbf{p}'-\mathbf{q}|i\rangle\ . \tag{27}$$

The first term gives rise to the plane-wave approximation, where the ejected nucleon is described by a free Dirac wave function and is not distorted by any nuclear potential. The second term is the modification caused by the final-state interactions of the ejected nucleon with the residual nucleus.

To evaluate Eq. (27), $G_0(p)$ is expanded into positive- and negative-energy solutions $|\mathbf{p},\alpha,\pm\rangle$ of the free Dirac equation for momentum $\mathbf{p}$

$$G_0(p)=\frac{1}{\gamma\cdot p-m_N+i\epsilon}$$
$$=\left[\sum_\alpha\frac{|\mathbf{p},\alpha,+\rangle\langle\overline{\mathbf{p},\alpha,+}|}{E-E_p+i\epsilon}+\frac{\sum_\alpha|\mathbf{p},\alpha,-\rangle\langle\overline{\mathbf{p},\alpha,-}|}{E+E_p+i\epsilon}\right], \tag{28}$$

where $E_p=(\mathbf{p}^2+m_N^2)^{1/2}$, m_N is the nucleon mass, $(+,-)$ denotes a (positive, negative) energy solution, and α labels the Pauli spin state. Upon inserting Eq. (28) into Eq. (27) and making use of the following notational assignments we have

$$\langle\overline{\mathbf{p},\alpha,\pm}|T_{\rm opt}(p,p';E)|\mathbf{p}',\beta,\pm\rangle=T^{\pm\pm}_{\alpha\beta}(p,p')$$
$$=\chi^\dagger_\alpha T^{\pm\pm}(p,p')\chi_\beta\ , \tag{29}$$

$$\langle\overline{\mathbf{p},\alpha\pm}|J^\mu(q)\langle\mathbf{p}-\mathbf{q}|i\rangle=J^\mu_{\alpha i}(q,\mathbf{p},\pm)\ , \tag{30}$$

where χ_α is a Pauli spinor. The second term of the virtual Compton amplitude of Eq. (27) becomes

$$\Delta T^{\mu\nu}\equiv\sum_i\int\frac{d^3p\,d^3p'}{(2\pi)^3}\left[J^\mu_{\alpha i}(q,\mathbf{p},+)^*\frac{1}{E-E_p+i\epsilon}T^{++}_{\alpha\beta}(p,p')\frac{1}{E-E_{p'}+i\epsilon}J^\nu_{\beta i}(q,\mathbf{p},'+)\right.$$
$$+J^\mu_{\alpha i}(q,\mathbf{p},+)^*\frac{1}{E-E_p+i\epsilon}T^{+-}_{\alpha\beta}(p,p')\frac{1}{E+E_{p'}-i\epsilon}J^\nu_{\beta i}(q,\mathbf{p}',-)$$
$$+J^\mu_{\alpha i}(q,\mathbf{p},-)^*\frac{1}{E+E_p-i\epsilon}T^{-+}_{\alpha\beta}(p,p')\frac{1}{E-E_{p'}+i\epsilon}J^\nu_{\beta i}(q,\mathbf{p}',+)$$
$$\left.+J^\mu_{\alpha i}(q,\mathbf{p},-)^*\frac{1}{E+E_p-i\epsilon}T^{--}_{\alpha\beta}(p,p')\frac{1}{E+E_{p'}-i\epsilon}J^\nu_{\beta i}(q,\mathbf{p}',-)\right]. \tag{31}$$

The evaluation of Eqs. (29)–(31) now proceeds as follows. In order to calculate R_L and R_T in a relativistic framework, the nuclear electromagnetic current operator is taken to be the free Dirac single-nucleon current operator

$$J^\mu(q)=F_1(q^2)\gamma^\mu+i\frac{F_2(q^2)}{2m}\sigma^{\mu\nu}q_\nu\ , \tag{32}$$

with form factors taken from Ref. 54 and modified as in Ref. 55. The Dirac momentum-space–bound-state wave functions $\langle\mathbf{p}-\mathbf{q}|i\rangle$ of Ref. 53 are then used to compute Eq. (30). No nonrelativistic p/m expansion of the current operator is employed.

As is apparent from Eqs. (29) and (31), T-matrix elements are needed at momenta "p" and "p'," which are off shell. In fact, it turns out that off-shell structure plays a significant role in determining the quasielastic response functions. The off-shell nucleon-nucleus T-matrix elements needed in Eq. (29) are calculated through the use of a relativistic Lippmann-Schwinger-type integral equation as detailed in Refs. 30 and 31. The code WIZARD, modified to accept an assortment of relativistic and nonrelativistic optical potentials and to generate fully off-shell T matrices, provides the needed T-matrix elements in partial-wave form.[30,31] The partial-wave T matrices are combined with partial-wave expansions of the $J^\mu_{\beta i}$ (see e.g., Ref. 44) to facilitate calculation of Eq. (31). A number of tests were performed to verify the numerical consistency and accuracy of the calculations, including comparisons with previous[14,15] results for real Hartree final-state interactions (FSI).

As is apparent in Eq. (31), quasielastic contributions arise not only from positive-energy, but also from explicit

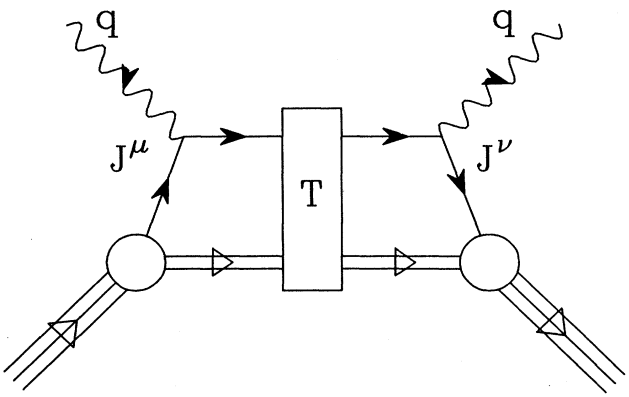

FIG. 1. Diagram of the final-state interaction contribution to the forward virtual Compton amplitude, which is the scattering of virtual photons from a nucleon in the nucleus. The "T" represents the final-state interaction between the ejectile and the residual nucleus. J^μ and J^ν are photonuclear electromagnetic vertices.

negative-energy T-matrix couplings. In fact, there are two distinct sources of such negative-energy contributions present in Eq. (31). Figure 1 shows a diagram of the virtual Compton amplitude. An explicit source of negative-energy contributions is manifest in the second, third, and fourth terms in Eq. (31). These terms involve T^{+-}, T^{-+}, and T^{--} and correspond to the physical situation where at least one virtual photon in Fig. 1 directly couples to a negative-energy nucleon channel at its vertex. The second source of negative-energy contributions arises implicitly through the T-matrix element T^{++} in the first term in Eq. (31). After the nucleon has been ejected from the nucleus, final-state interactions represented by "T" in Fig. 1 couple the nucleon to negative-energy channels in intermediate states. In other words, the integral equation that determines T^{++} contains couplings to negative-energy intermediate states through the Dirac optical potential. The practical significance of these two types of negative-energy contributions for the quasielastic response functions is detailed in the next section.

IV. RESULTS

Representative results of extensive calculations of the longitudinal and transverse response functions for the inclusive quasielastic (e,e') reaction, within the context of (16c), are presented in Figures 2–16. In this paper, we are basically interested in physically observable effects (and their character) which may arise from final-state interactions. To study such FSI effects in detail, nonrelativistic and relativistic dynamic calculations have been performed within the context of a number of models and with the capability of isolating several distinct physical processes. Results are shown for slices through the q-ω plane, as a function of ω for three fixed q values: $q=410$ MeV/c, $q=550$ MeV/c, and $q=700$ MeV/c. Since the point of our study is to explore the physical implications of a variety of theoretical and phenomenological treatments of the FSI, no adjustable parameters are used, either in the microscopic theoretical or in the phenomenological models. Even for the lowest momentum transfer, $q=410$ MeV/c, the quasielastic peak occurs at $\omega > 100$ MeV, so that microscopic multiple scattering theory should be reasonably applicable, especially at and above the peak. Of course, as ω decreases below 80–100 MeV, the microscopic theory becomes increasingly untenable and phenomenology must be relied upon. Thus the quasielastic calculations associated with microscopic multiple-scattering optical potentials should not be taken too seriously for small ω.

For each relativistic and nonrelativistic calculation, the corresponding "on-shell" and plane-wave limits are isolated for comparison. The plane-wave limit is the result of (16c) when there are no FSI, that is when $T_{\rm opt}\equiv 0$. The calculation which is referred to as "on-shell" incorporates into (16c) only the on-shell part of $T_{\rm opt}$ (see Sec. III).[44] The momentum-space matrix elements of $T_{\rm opt}$ involve initial and final momenta, $\mathbf{p}'$ and $\mathbf{p}$, corresponding to energies generally different from the parametric energy E of $T_{\rm opt}(E)$, which specifies the energy of the asymptotic ejected nucleon. Off-shell kinematics is the general circumstance, since only when all three of these energies coincide is $T_{\rm opt}(E)$ on shell, [i.e.,

$$E=(\mathbf{p}^2+m_N^2)^{1/2}=(\mathbf{p}'^2+m_N^2)^{1/2}] \ .$$

The distinction between on-shell FSI effects and those which appear exclusively off-shell is important because the former are observable in elastic proton scattering and are thus much more securely known. The off-shell behavior of $T_{\rm opt}$ is typically extrapolated using some theoretical ansatz, such as meson theory. In the present case of quasielastic electron scattering effects which derive from the on-shell part of $T_{\rm opt}$ are on a very solid footing. The purely on-shell calculation is also of interest because the various models which we investigate do not precisely agree in their on-shell predictions for $T_{\rm opt}$, a defect which should in principle be remedied by minor parametric adjustments within the models. Comparison of the quasielastic predictions of the various models in conjunction with a comparison of their corresponding on-shell limits then enables one to gauge the degree to which differing quasielastic predictions made by the models reflect their intrinsic dynamical differences rather than just their differing precisions in describing the known on-shell amplitude.

In the nonrelativistic case the quasielastic predictions of phenomenology, impulse approximation and local density approximation (LDA) treatment of the FSI are compared. These are then contrasted with corresponding predictions made on the basis of several relativistic models. The relativistic models of the FSI employed include a microscopic impulse approximation optical potential, a global energy-dependent phenomenological parametrization and a (Hermitean) Hartree potential.

In the relativistic dynamical calculations two sources of negative-energy contributions or virtual pair effects are isolated. The explicit source involves direct vertex couplings by $T_{\rm opt}$ to negative-energy states, represented by

the last three terms in Eq. (31). Turning off these explicit pair effects yields a calculation referred to as NEP (no explicit pair effects). Even if only positive-energy matrix elements of $T_{\rm opt}$ are used, virtual pair effects still derive from the integral equation[31] used to obtain $T_{\rm opt}$ from $V_{\rm opt}$. If, in addition to neglecting the explicit negative-energy contributions, pair effects are turned off in the integral equation, a calculation referred to as NP (no pair effects) is obtained. This is a purely positive-energy limit, in the sense that all Dirac sea effects are removed. The capability to perform these distinct calculations allows us to isolate and uncover the exact source of specific pair effects seen in the quasielastic predictions. The NP limit must be used with some care since turning off pair effects in the integral equation for $T_{\rm opt}$ will produce a different on-shell scattering amplitude. Nevertheless, to the extent that the on-shell $T_{\rm opt}$ are not markedly different, the NP limit defines a useful corresponding nonrelativistic limit.

Before discussing individual figures there are several general results that can be inferred globally from the figures. First, in each figure the relativistic plane-wave calculation is shown as a reference curve. The corresponding nonrelativistic calculation is not shown in any of the figures, since the two plane-wave calculations are virtually identical. The input to these calculations differs only in the presence or absence of negative-energy components in the bound states. As discussed in Sec. II C, there is no ambiguity introduced by differing current operators, thus virtual pairs (negative-energy components) in the bound-state wave functions are completely negligible as far as quasielastic (e,e') is concerned, at least in areas of the q-ω plane where the longitudinal and transverse response functions are appreciable.

Second, FSI are never neglectable. In no case is the plane-wave approximation adequate. Similarly, off-shell FSI effects are found always to be qualitatively important. FSI always suppress the peak heights of both response functions considerably and the size of this effect is dynamically dependent as is the relative effect on the transverse and longitudinal response functions. Because of the unitary nature of Eqs. (16) and (18) and in accord with the nonrelativistic Coulomb sum rule, the strength subtracted from the peaks by the FSI is largely dispersed to the high-energy tails of the distribution, broadening it considerably. Thus, the effect of the FSI is mainly to redistribute the quasielastic strength in the q-ω plane, changing the overall shape of the distribution. The character of the various dynamical calculations with regard to the Coulomb sum rule is discussed in detail elsewhere,[56] here it is simply noted that our various results typically saturate the sum rule to within about 10%. Our immediate conclusions are thus: (1) Proper inclusion of FSI is crucial for meaningful comparison of theoretical results with experimental data; (2) The direct physical approach of (16) provides an advantageous framework for analyzing FSI effects in inclusive quasielastic (e,e'); and, in addition, (3) Off-shell FSI effects are invariably important, can never be neglected or approximated away, and show considerable sensitivity to the theoretical model employed.

Finally, the various models differ greatly in the degree of their agreement with the experimental data for the transverse and longitudinal response functions, although several characteristic trends can be discerned, as is discussed later. Nevertheless, the general result is that in no case is simultaneous agreement between theory and experiment for both response functions found. The implications of this failure, and the way it occurs in the various models, is discussed in detail later.

A. Nonrelativistic FSI results

Figures 2(a) and (b) compare several nonrelativistic calculations at a momentum transfer of 410 MeV/c for R_L and R_T, respectively. The short-dashed curves correspond to an optically factorized impulse approximation (IA) optical potential[30] using Franey-Love N-N amplitudes[57] and the dot-dashed lines to an IA optical potential using Franey-Love amplitudes in the local $t(q)\rho(q)$ approximation.[26] The solid curves correspond to a local density approximation (LDA) optical potential constructed using Bonn N-N amplitudes.[29] The predictions of a nonrelativistic, phenomenological, energy-dependent, Woods-Saxon potential fitted[28] to proton scattering data is also displayed in Fig. 2 as the long-dashed curve. In Figs. 2a and b there is a dramatic difference between the plane-wave calculation and the others. The FSI greatly reduce the quasielastic peak heights, broaden the distributions, shift the position of the peaks, and enhance the high- and low-energy tails of both response functions.

The two nonrelativistic IA calculations make very similar quasielastic predictions. Apparently, differing IA prescriptions result in little quasielastic (e,e') ambiguity once the input two-body amplitudes are specified. The predictions of the phenomenological optical potential are quite different, being much less suppressed relative to the plane-wave limit at the quasielastic peak. This dichotomy is easily understood on the basis of results from elastic proton scattering, where the absorptive potentials predicted by the IA tend to be considerably stronger than those obtained from phenomenology.[33] The elastic proton data of course favors the phenomenological potential; however, elastic predictions are somewhat insensitive to such differences due to the fact that black-disc scattering dominates and further increases in the "blackness" in the nuclear interior are relatively unimportant. Evidently the quasielastic (e,e') reaction is more sensitive to the character of the absorptive potential. Stronger absorption further depletes the quasielastic strength relative to the plane-wave prediction at the quasielastic peak. In view of the unitary nature of Eq. (16) the strength drained from the plane-wave response by the absorptive potential is then shifted in the q-ω plane to broaden the distributions and enhance their tails. LDA optical potentials typically display greater similarity to phenomenological potentials than do IA optical potentials. This is due to LDA density corrections which significantly suppress the imaginary potentials[26,29] and is consistent with the close agreement seen in Fig. 2 for the quasielastic (e,e') predictions made by the LDA and phenomenological optical models.

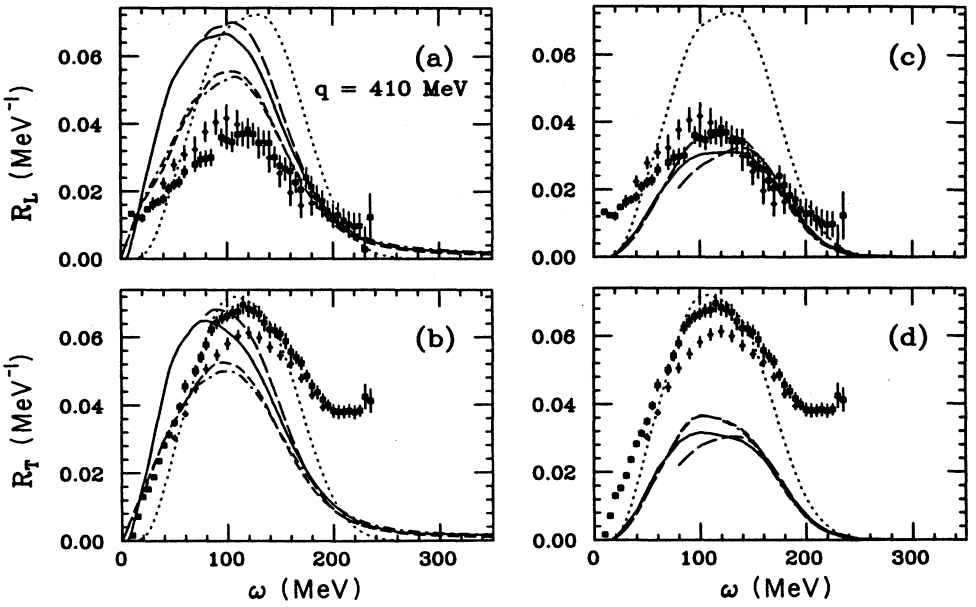

FIG. 2. The longitudinal (a) and transverse (b) response functions for ^{40}Ca at $q = 410$ MeV/c as a function of energy transfer, ω. Calculations are shown for the free relativistic plane-wave approximation with no final-state interactions (dotted line), the nonrelativistic LDA with Bonn N-N amplitudes (solid line), the nonrelativistic IA with Franey-Love N-N amplitudes (dot-dashed line), the nonrelativistic optimally factorized IA with Franey-Love amplitudes (short-dashed line), and the nonrelativistic Woods-Saxon fit (long-dashed line). (c) and (d) are the same as (a) and (b), respectively, except only the on-shell contributions from T_{opt} are included in the calculations. The data are from Ref. 4 (solid diamonds) and Ref. 3 (open boxes).

The nonrelativistic on-shell results, shown in Figs. 2(c) and (d), are very similar in size and shape, supporting the earlier claim that the on-shell matrix elements of the various T_{opt} are much better constrained. It would be very suprising if this were not the case. In comparison with the full calculation the on-shell curves are greatly suppressed, emphasizing the importance of off-shell contributions. The large differences observed in the full calculations are not reflected in the on-shell results, indicating that these effects are due to the different off-shell extensions of T_{opt}. Also, the high-energy tails in the full calculations are seen to be solely the result of off-shell contributions, as expected.

In Fig. 3 analogous calculations are shown at a momentum transfer of 500 MeV/c. Although these figures show much the same qualitative features as in Fig.

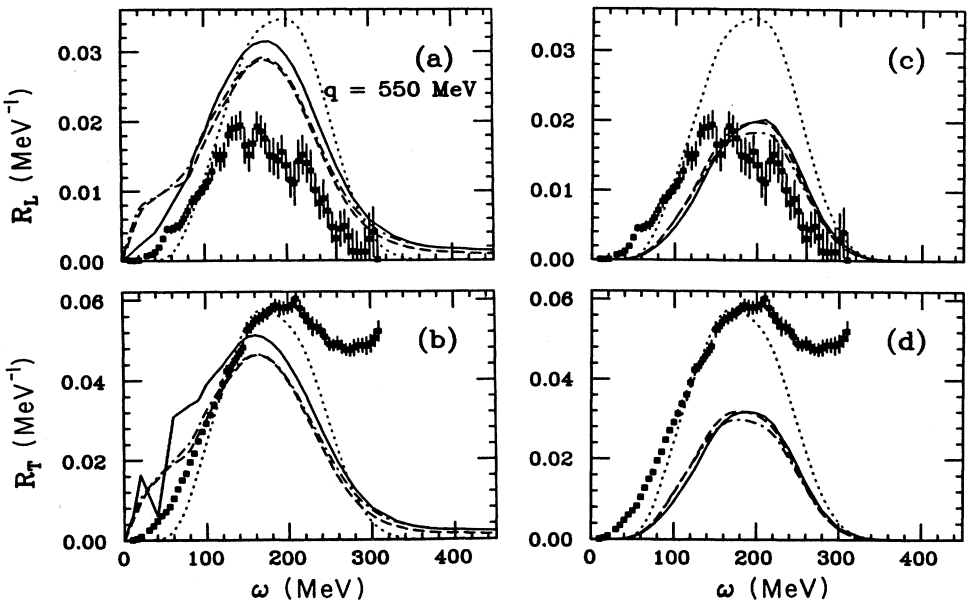

FIG. 3. (a) and (b) are the same as in Fig. 2 except at $q = 550$ MeV/c. (c) and (d) are the same as (a) and (b), respectively, except only the on-shell contributions from T_{opt} are included in the calculations.

2, the differences among the various calculations are much smaller. The two IA calculations are again very close together, showing almost identical results. The LDA calculation is now much closer to the other calculations than it was at 410 MeV/c. This is consistent with the behavior of LDA modifications to the N-N amplitudes, which fall as the energy increases or as the momentum transfer increases at fixed energy. Figure 3 also suggests that at higher momentum transfer reasonable nonrelativistic FSI may display less variability in their quasielastic (e,e') predictions. Results for the phenomenological potential used in Fig. 2 are not shown here because of the restricted range of validity of this potential.

The nonrelativistic FSI suppress the peak heights (relative to the corresponding plane-wave calculation) of both response functions. In comparing the effect on the two response functions, the suppression of R_T is slightly greater than that for R_L. This is a consistent feature of our calculations that is not at all in agreement with the trend observed in the experimental data. While suppression of the peak height of R_L is needed for agreement with the data, the FSI-induced suppression is too small by a factor of about 2. Moreover, in the case of R_T, little if any suppression is apparently required by the data, while the predictions using realistic FSI imply is suppression of about 20%. However, this latter contradiction need not be taken too seriously since it is evident from the data that much more transverse strength is present in (and below) the dip region above the quasielastic peak, and that this strength is large enough to affect R_T at its peak.[58] Whatever the source of this additional strength, it is then clear that it can appreciably enhance the quasielastic peak so that appropriate FSI suppressions of R_T will ultimately play an important role in achieving theoretical consistency with the R_T data. In this regard, it is important to emphasize that the transverse anomaly can have absolutely nothing to do with validating, in any sense, a plane-wave treatment for R_T. All of the transverse quasielastic strength contained in the plane-wave limit is present in the treatment of Eq. (16c) of the FSI, by virtue of its unitary character in the P_{α_i} space as expressed, for example, by Eq. (18). This is made obvious by writing Δg in Eq. (18) in its (biorthogonal) spectral form and noting that the energy integral then just reproduces the one-body–plane-wave completeness relation. Thus, the effect of the FSI is to redistribute the transverse strength in the q-ω plane by dispersive processes which, physically, must be present. Whatever the additional physical mechanism responsible for the observed enhancement of the transverse quasielastic peak, it must be in addition to the physics contained in the nonrelativistic optical model treatment of the P_{α_i} space and thus physically has nothing to do with the plane-wave limits. Finally, in contrast to the transverse case, the shape of the longitudinal quasielastic peak appears to be in qualitative agreement with the data. The nonrelativistic FSI systematically overestimate the peak heights of R_L as found in earlier calculations.[59]

Within the nonrelativistic framework final-state interactions cause large effects, producing various shape modifications and significantly suppressing both response functions relative to the plane-wave approximation, with the suppression of R_T larger than that of R_L. Differences between the various FSI results arise primarily from the differing off-shell behaviors of $T_{\rm opt}$, as determined by the optical potentials used to describe the FSI. Also, the Green's function doorway approach (GFDA) is very sensitive to the non-Hermitian (absorptive) potentials, with the amount of suppression near the quasifree peak directly related to the magnitude of the absorptive potential. At higher momentum transfers the different FSI models yield results which tend to converge. In this nonrelativistic analysis, even though the shape of R_L is in qualitative agreement with the data, the longitudinal suppression is inadequate by a factor of 2 to recover the data.

B. Relativistic versus nonrelativistic FSI results

In discussing the figures individually it is now convenient to make some global symbolic assignments of curve types. In the following figures the dotted curve denotes the relativistic plane-wave calculation for the relevant value of q. Dot-dashed curves represent the on-shell limit of the calculation depicted as a dashed curve in the same figure, with short or long dashes being used to distinguish between different sets of curves.

Quasielastic predictions made on the basis of two relativistic dynamical descriptions of the FSI are displayed in Figs. 4 and 5 at momentum transfers of 410 MeV/c and 550 MeV/c, respectively. In each figure the long-dashed line denotes the prediction based on the global, phenomenological energy-dependent, relativistic optical potential of Ref. 35, while the short-dashed curve denotes the microscopic relativistic IA optical potential of Ref. 31. The former is simply referred to as the "relativistic global" FSI. The corresponding on-shell calculations are also shown and are denoted in accord with the convention described earlier. In both figures and for both FSI the importance of the redistribution of strength caused by the FSI, which reduces the quasifree peak and enhances the tails of the distributions, is again observed. Quantitatively, however, the trends are somewhat different than for the nonrelativistic dynamics. In Fig. 4 the suppression of the longitudinal quasifree peak (relative to the plane-wave prediction) by the relativistic FSI is about 26% for the global potential and about 38% for the IA potential. Similarly, the suppression of the transverse response is about 19% for the global potential and about 32% for the IA potential. The same pattern is found at $q=550$ MeV/c in Fig. 5, with the peak longitudinal response producing a reduction of about 27% for the global potential and about 32% for the IA optical potential, while the suppression of the transverse response is about 22% for the global potential and about 25% for the IA potential. Thus, in all of the relativistic dynamical calculations the suppression of the longitudinal is slightly greater than the suppression of the transverse quasielastic response. This is opposite to the trend observed for the quasielastic response based upon nonrelativistic dynamics.

The IA predictions for the longitudinal response are

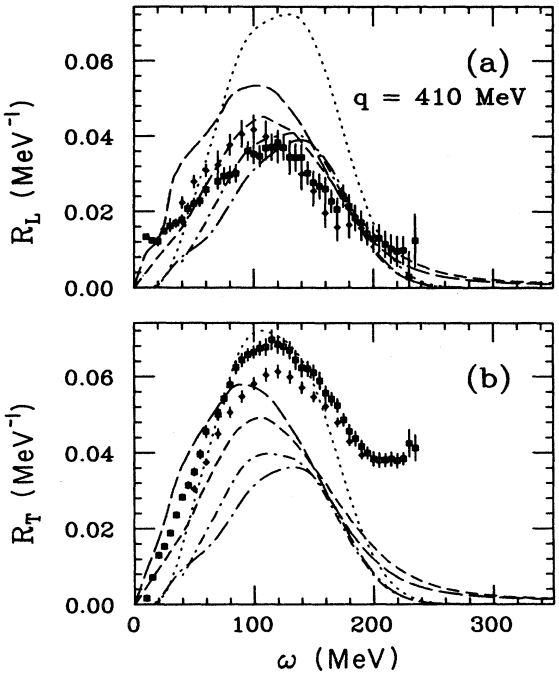

FIG. 4. Longitudinal (a) and transverse (b) response functions for ^{40}Ca at $q = 410$ MeV/c as a function of energy transfer, ω. Calculations are shown for the relativistic free plane-wave approximation (dotted line), Dirac global phenomenology (long-dashed line), and the Dirac IA (short-dashed line). On-shell curves are also displayed, where Dirac global phenomenology (dot-long-dashed line) and the Dirac IA (dot-short-dashed line) are used.

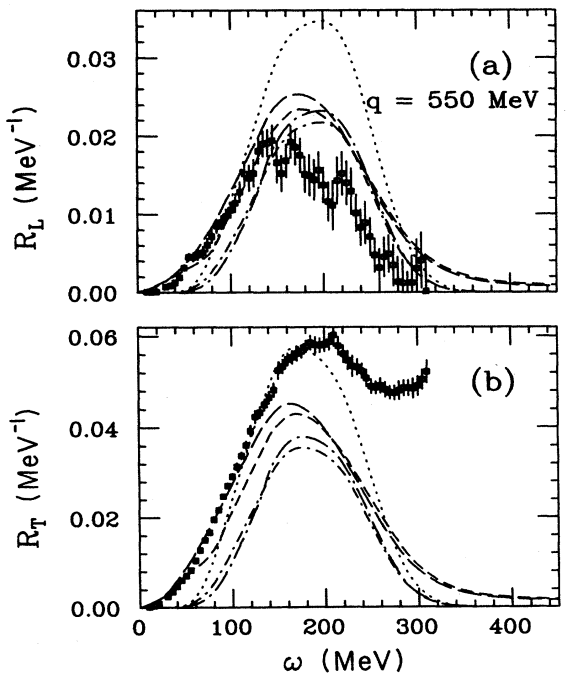

FIG. 5. The same as Fig. 4, except at 550 MeV/c momentum transfer.

now in good agreement with the data at 410 MeV/c and are approaching agreement at 550 MeV/c. The correspnding predictions of the global potential do not fare quite so well, considerably overpredicting the peak strength at both q values. The IA predictions also graphically emphasize that it is the relative R_L-R_T peak size which needs to be understood, not simply a suppression of R_L, because the agreement with R_L is good while R_T is inexplicably large. Too much should not be made of this, however, since the reasons for the difference between the predictions of the relativistic global and IA FSI are not clear. On the other hand, this change of focus, from an apparent suppression of R_L to an apparent enhancement of R_T, receives some support from recent exclusive measurements where an unexplained enhancement of R_T was observed.[58] The on-shell predictions do not reflect any systematic deviations. The two relativistic potentials yield similar, but not identical on-shell results. At 410 MeV/c Fig. 4 reveals that most of the differences between the predictions of the two potentials is due to differing off-shell contributions. The opposite is true at 550 MeV/c in Fig. 5 in that the differences appear to be primarily on-shell in nature. This can be attributed to the fact that at higher momentum transfers (and therefore higher ejected nucleon energies) more and more of the strength is near the on-shell limit, as should be expected. Finally, it is noted that there exists a qualitative agreement between the relativistic dynamical predictions and the data, particular for both tails of the longitudinal distribution, and the low-energy tail of the transverse response.

It has already been noted that the nonrelativistic FSI tend to suppress R_T slightly more than R_L (relative to the plane-wave approximation), while the relativistic FSI suppress R_L more than R_T. To better observe these relative suppressions, representative quasielastic predictions of the relativistic and nonrelativistic dynamical models are explicitly compared in Figs. 6–9. Figures 6 and 7 compare the predictions made by the relativistic global FSI to those of the nonrelativistic LDA optical potential at 410 MeV/c and 550 MeV/c, respectively. The nonrelativistic LDA calculation was seen in Figs. 2 and 3 to be representative of nonrelativistic phenomenology at 410 MeV/c and of generic nonrelativistic results at 550 MeV/c. Figures 8 and 9 compare the $|\mathbf{q}| = 410$ and 550 MeV/c quasielastic predictions made by the microscopic relativistic and nonrelativistic IA optical potentials of Refs. 30 and 31. The corresponding on-shell limits are shown for all of these cases. Although the on-shell predictions shown in the comparisons of Figs. 6–9 do show some differences in detail, it is clear that this is not the effect of primary importance. In all four figures, at the quasielastic peak, the additional suppression of the longitudinal response due to relativistic dynamics is much larger than the additional relativistic suppression found for the transverse response. In fact, the relativistic suppression of R_L is about 20% whereas the corresponding suppression of R_T is on the order of 10% or less. Purely nonrelativistic FSI dramatically suppress R_T relative to R_L at the quasifree peak, while the converse is true with added relativistic FSI dynamics. Thus, rela-

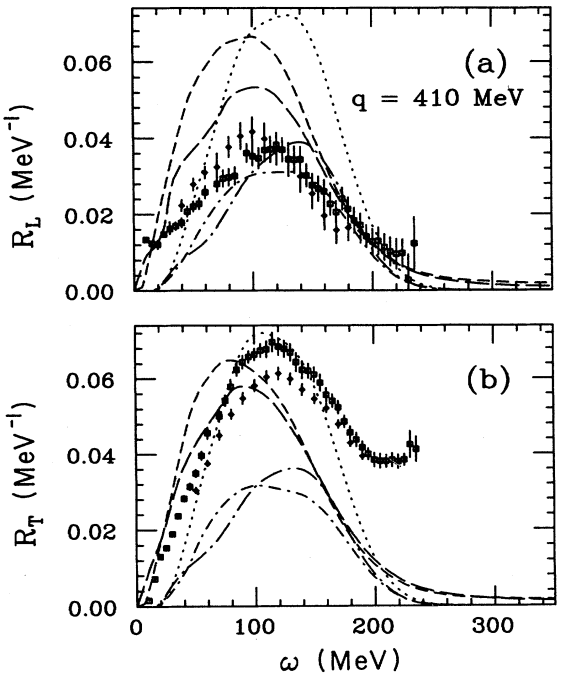

FIG. 6. Longitudinal (a) and transverse (b) response functions for ^{40}Ca at $q = 410$ MeV/c as a function of energy transfer, ω. Calculations are shown for the relativistic free plane-wave approximation (dotted line), Dirac global phenomenology (long-dashed line), and the nonrelativistic LDA with Bonn N-N amplitudes (short-dashed line). On-shell curves are also displayed, where Dirac global phenomenology (dot-long-dashed line) and nonrelativistic LDA with Bonn (dot-short-dashed line).

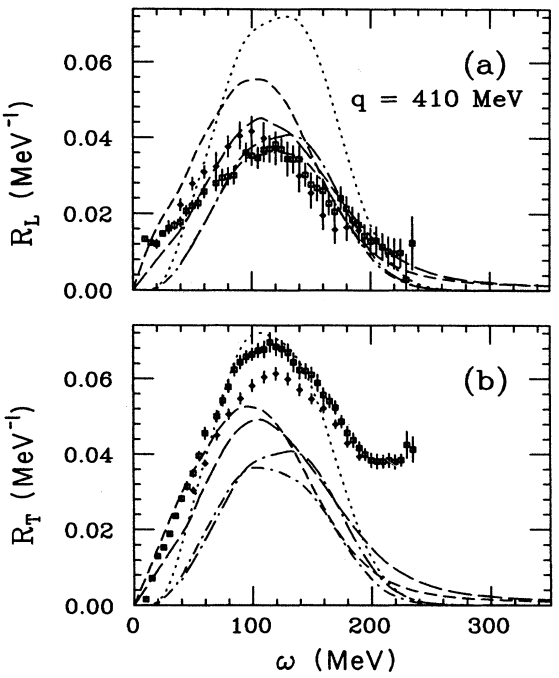

FIG. 8. Longitudinal (a) and transverse (b) response functions for ^{40}Ca at $q = 410$ MeV/c as a function of energy transfer, ω. Calculations are shown for the relativistic free plane-wave approximation (dotted line), the Dirac (long-dashed line), and the nonrelativistic (short-dashed line) optimally factorized IA with Franey-Love amplitudes. On-shell curves are also displayed, for the Dirac (dot-long-dashed line) and nonrelativistic IA with Franey-Love amplitudes (dot-short-dashed line).

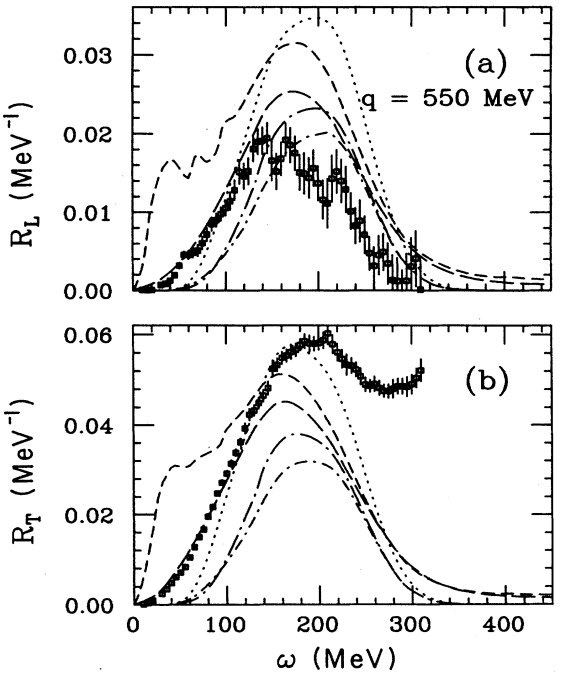

FIG. 7. The same as Fig. 6, except at 550 MeV/c momentum transfer.

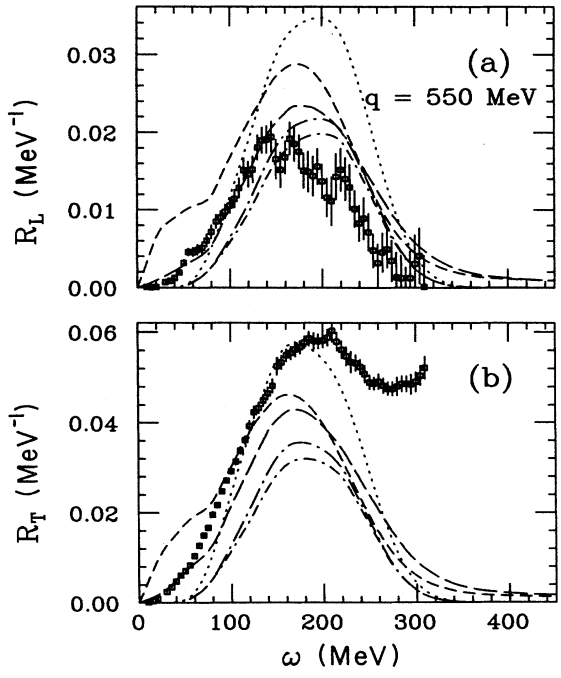

FIG. 9. The same as Fig. 8, except at 550 MeV/c momentum transfer.

tivistically, the transverse response function is reduced slightly, while the longitudinal response is suppressed significantly towards the data. If the relativistic global FSI are compared directly with the nonrelativistic IA predictions, the longitudinal response is suppressed by 3% at $|\mathbf{q}|=410$ MeV/c and 11% at $|\mathbf{q}|=550$ MeV/c, while R_T is enhanced by 11% at $|\mathbf{q}|=410$ MeV/c and suppressed by about 2% at $|\mathbf{q}|=550$ MeV/c. In this case the phenomenological evidence is overwhelmingly in favor of including relativistic dynamics. In comparing the on-shell-only results in Figs. 6 and 7 there does not appear to be any systematic behavior, while in Figs. 8 and 9 some of the trends observed in the full calculations can be traced to the on-shell contributions. The on-shell effects are not very large, and it is clear that the main effects are due to the off-shell behavior of $T_{\rm opt}$.

In this section we found the relativistic FSI approach provides a much more realistic description of the data than does the nonrelativistic theory. The suppression caused by relativistic FSI in comparison with the relativistic plane-wave result is much larger than that found in the nonrelativistic case, with the longitudinal suppression consistently greater than the transverse suppression. In comparing relativistic FSI results directly with the nonrelativistic FSI calculations, the longitudinal response is suppressed twice as much as is the transverse response. Phenomenologically, the trends seen here support the inclusion of Dirac degrees of freedom. The origin of the observed relativistic FSI effects is clarified in the next set of figures.

C. Negative-energy contributions

Physically, the main differences between the relativistic and nonrelativistic calculations are the contributions that arise due to negative-energy channel effects in the relativistic optical potentials and T matrices. Figures 10–12, for $q=410$ MeV/c, 550 MeV/c, and 700 MeV/c, respectively, resolve the global relativistic quasielastic predictions into their component parts. As described earlier, the negative-energy contributions can be ascribed to two categories. The NEP calculation includes virtual pair effects used in the construction of the positive projection of $T_{\rm opt}$, while excluding explicit negative-energy state couplings by $T_{\rm opt}$. The full calculations are depicted by the long-dashed line and the corresponding NEP and NP calculations by the solid and short-dashed curves, respectively. Associated on-shell limits follow our standard convention and again the differing on-shell FSI effects are not of essential importance. Because the NP limit is reached by turning off all final-state pair effects, it may be regarded as something of a nonrelativistic limit of the global relativistic calculation. If the global NP limits are compared with the nonrelativistic predictions of the preceding set of figures, Figs. 6–9, the off-shell differences between these two "nonrelativistic" calculations account for about 50% of the additional relativistic suppression of R_L seen in Figs. 6–9 and essentially all of the additional suppression of R_T. For R_L turning off only the explicit pair contributions reduces the suppression of the quasielastic peak. Turning off the remaining

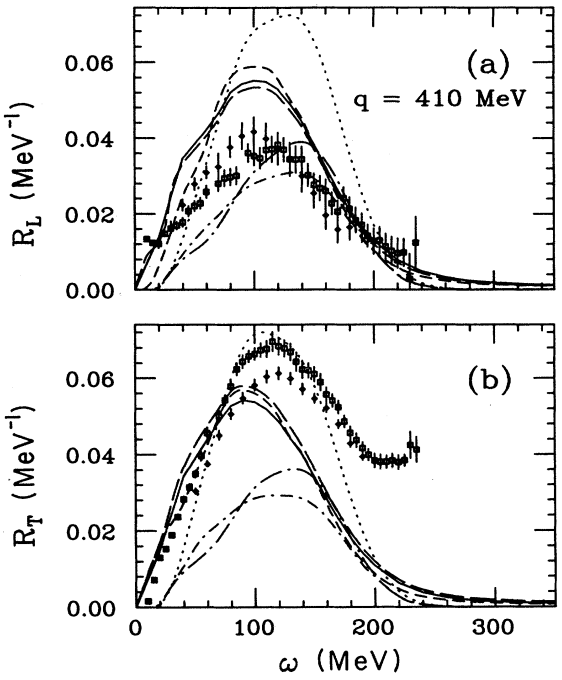

FIG. 10. Longitudinal (a) and transverse (b) response functions for ^{40}Ca at $q=410$ MeV/c as a function of energy transfer, ω. The relativistic free plane-wave approximation (dotted line) calculation is shown along with calculations using Dirac global phenomenology to describe the FSI. The full Dirac calculation (long-dashed line), the pure positive-energy NP calculation (short-dashed line), and the NEP calculation with no explicit negative-energy terms in Eq. (31) (solid line) are shown along with on-shell calculations with (dot-long-dashed line) and without (dot-short-dashed line) negative-energy contributions.

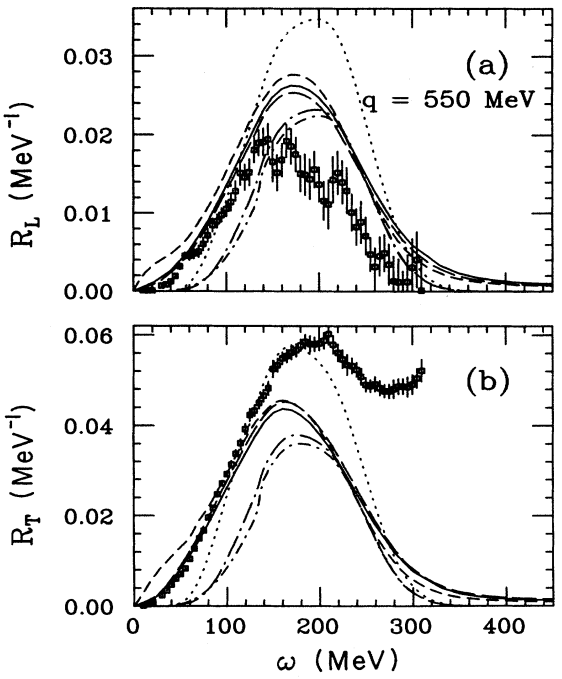

FIG. 11. The same as Fig. 10, except at 550 MeV/c momentum transfer.

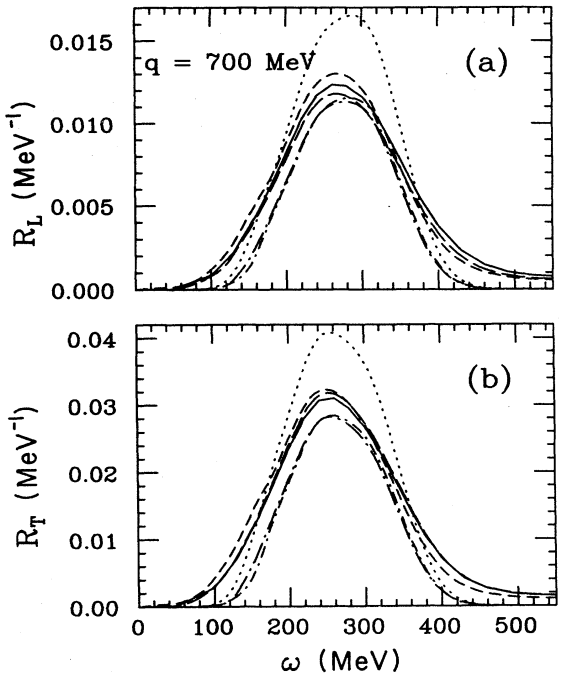

FIG. 12. The same as Figs. 10 and 11, except at 700 MeV/c momentum transfer.

pair contribution (virtual pairs in intermediate states in the integral equation for $T_{\rm opt}$), in addition, further reduces the suppression. Thus for R_L both pair contributions suppress the peak quasielastic strength. For R_T the trends are somewhat different, with turning off the explicit pair contributions suppressing the quasifree peak. Turning off the remaining pair contributions then effectively cancels this effect. Thus for R_T explicit pair contributions enhance the quasielastic peak, but this is canceled by the suppressive effect of the remaining pair contributions. The net result is that off-shell effects of a nonrelativistic type account for half of the relativistic suppression of R_L and all of the relativistic suppression of R_T. Manifest pair contributions account for half of the relativistic suppression of R_L, but have little effect on R_T. The net effect seen due to negative-energy contributions is typical of all relativistic potentials examined.

As a side note a very interesting trend is seen in Figs. 10, 11, and 12, involving the off-shell contributions. As the momentum transfer $|\mathbf{q}|$ is increased, the predicted response functions are increasingly well represented by their on-shell limit. This is not a surprising result, and in Figs. 12(a) and (b) the on-shell-only curves are almost the same size as the full curves. However, the large high-energy tail and shape modifications due to off-shell effects remain even at 700 MeV/c. Within the nuclear medium the final-state interactions shift the ejected nucleon off-shell, but as the momentum transfer increases, the ejected nucleon becomes relatively less affected by medium effects near the quasielastic peak. However, the tails always depend upon momentum-transfer sharing with the FSI so that even at $|\mathbf{q}|=700$ MeV/c there is still a significant off-shell effect.

For all cases considered, negative-energy Dirac sea effects cause a systematic suppression of R_L while leaving R_T relatively unchanged.

D. Effects due to non-Hermiticity

Figures 13–16 investigate the effect of non-Hermitean FSI on the quasielastic response functions. Figures 13–15 compare, at $q=410$ MeV/c, 550 MeV/c, and 700 MeV/c, respectively, the quasielastic predictions associated with the global relativistic optical potential (long-dashed), and those obtained from a Hermitean relativistic Hartree potential (solid).[53] Also shown in these figures is a comparison of the quasielastic predictions of the NP "nonrelativistic" limit for both the Global (short-dashed) and Hartree (dot-dashed) FSI. As is to be expected, because the Green's function formalism preserves the completeness relation on the one-body space, no dramatic reduction in overall quasielastic strength results from non-Hermitean optical potentials. Rather, the effect of the non-Hermiticity is, and can only be, to provide a somewhat different dispersive mechanism through which to redistribute the quasielastic strength. This is discussed in more detail relative to the Coulomb sum rule elsewhere.[56] As is evident in Figs. 13–15, for the peak of the longitudinal response, where the relativistic effects are larger than for the transverse case, the non-Hermitean

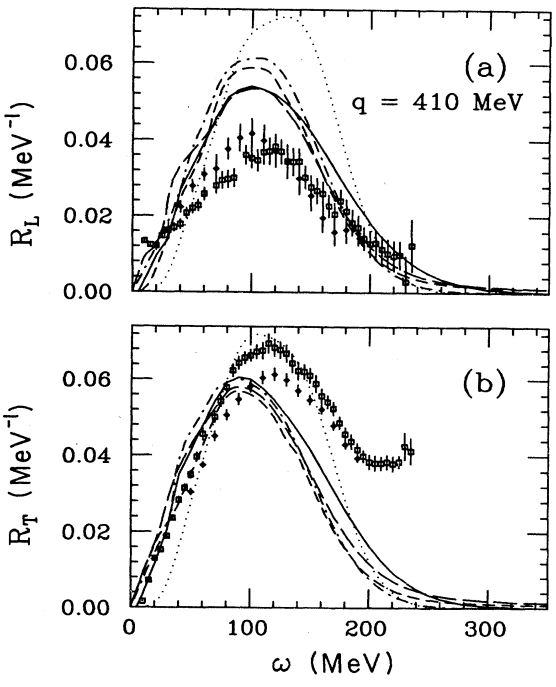

FIG. 13. Longitudinal (a) and transverse (b) response functions for ^{40}Ca at $q=410$ MeV/c as a function of energy transfer, ω. The relativistic free plane-wave approximation calculation (dotted line) is shown along with calculations using Dirac global phenomenology in full Dirac (long-dashed line) and positive-energy NP (short-dashed line) format, and using relativistic Hartree potentials in full Dirac (solid line), and positive-energy NP (dot-dashed line) format.

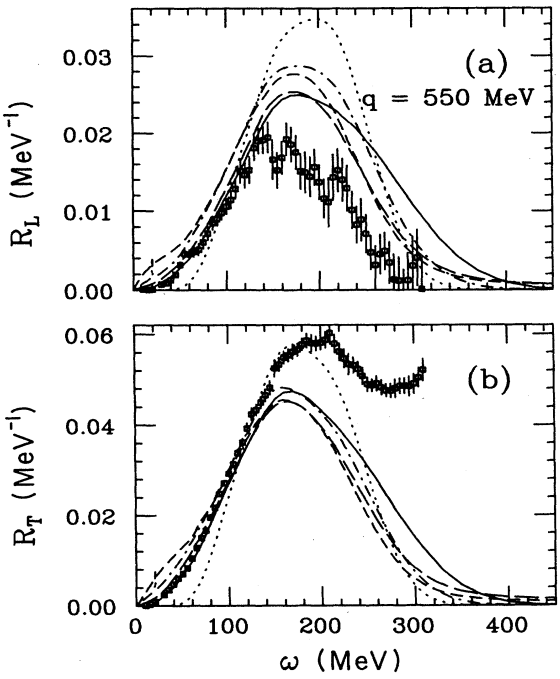

FIG. 14. The same as Fig. 13, except at 550 MeV/c momentum transfer.

effects are much smaller than the differences between relativistic and NP "nonrelativistic" predictions. For the transverse response, however, non-Hermitean effects are somewhat larger at the quasielastic peak. It is clear from these figures that there is a systematic difference in shape between the energy-dependent, non-Hermitean, global

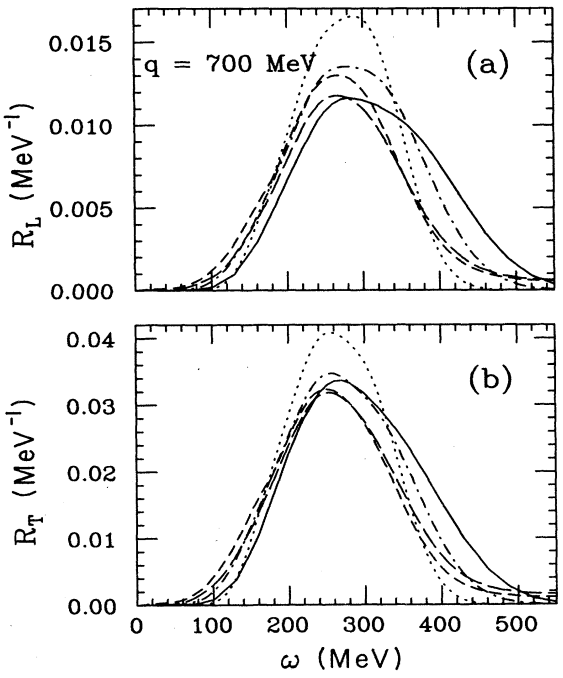

FIG. 15. The same as Fig. 13, except at 700 MeV/c momentum transfer.

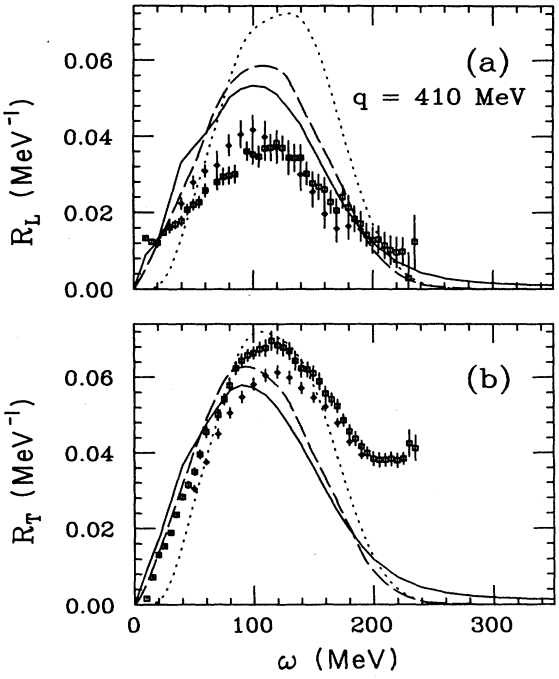

FIG. 16. Longitudinal (a) and transverse (b) response functions for ^{40}Ca at $q = 410$ MeV/c as a function of energy transfer, ω. The relativistic free plane-wave approximation calculation (dotted line) is shown along with calculations using Dirac global phenomenology to describe the FSI. The full Dirac calculation (solid line) and a calculation, where only the real part of the sane optical potential (dashed line) is used, are shown.

optical potential and the energy-independent, Hermitean, Hartree potential for both relativistic and nonrelativistic dynamics. The response functions for the Hartree potential are noticeably broader than the corresponding response functions for the global potential. Since the integrated strength should be roughly the same for Hermitean and non-Hermitean potentials, the response functions for the global potential have a much larger high-energy tail than those for the Hartree potentials, which compensates for the relatively narrow quasielastic peak. These differences in shape become more pronounced with increasing momentum transfer.

In comparing the shapes of the quasielastic peaks calculated with the energy-independent Hartree and the global energy-dependent phenomenology, it is apparent that the energy dependence of the potentials is important. The energy dependence is related to the analytic structure of the optical potential, where the real and imaginary parts are connected through a dispersion relation. Energy dependence also arises from the nonlocal structure of the optical potential. It is apparent that the quasielastic response functions calculated in the optical model approach are sensitive to the energy dependence of the optical potential.[25,26]

Finally, the full relativistic global calculation (solid line) is compared in Fig. 16 to predictions from an otherwise identical calculation in which the non-Hermitean part of the Dirac global optical potential is turned off

(dashed line). Here, as might be expected, the observed effects of the non-Hermiticity on the quasielastic response are more distinctive, with the quasifree peaks showing an appreciable suppression due to non-Hermitean FSI. Of course, the associated enhancement of the tails of the distribution by the non-Hermitean FSI is also seen. Thus, Fig. 16 provides a more direct confirmation of the characterization of non-Hermitean effects inferred from Figs. 13–15.

Non-Hermitean FSI cause a redistribution of strength within the quasielastic peak. Although the gross features of quasielastic electron scattering can be mimicked by modifications to purely Hermitean, energy-independent FSI, additional nontrivial features, such as a narrower peak and a much larger, more extended high-energy tail, are produced by a physically realistic energy-dependent complex optical potential. For a microscopic description of the quasielastic response it is necessary to properly incorporate the reactive content represented by the non-Hermiticity and energy dependence of the optical potential.

V. SUMMARY AND CONCLUSIONS

In this paper a microscopic theoretical, Green's-function formalism for analyzing the response functions of the inclusive quasielastic (e,e') reaction has been reviewed, developed, and applied. This formalism properly incorporates the non-Hermitean potentials needed to reflect inelastic multistep and absorptive processes. The Green's-function formalism provides a conceptually clear framework for treating the quasielastic inclusive reaction that goes far beyond simple plane-wave or Hermitean potential models, permitting a relatively clear identification of approximations and appropriate corrections. The formalism also provides an advantageous numerical framework for analyzing FSI, relativistic dynamics, and other mechanisms relevant to inclusive quasielastic (e,e'). A number of relativistic and nonrelativistic dynamical models of the final-state interactions have been examined for the case of ^{40}Ca. This was done in a manner which allowed for the isolation of several distinct dynamical mechanisms. A number of conclusions can be inferred from these investigations.

(1) FSI effects can never be neglected or approximated away. For meaningful comparisons with the data, FSI are essential; plane-wave approximations are never adequate. The FSI serve to suppress the heights of the peaks for both quasielastic response functions and transfer strength to the tails of the distributions. Off-shell scattering dynamics, which is not well constrained by elastic proton scattering, determines the q-ω distribution of approximately 50% of the response functions. Differing off-shell behaviors of the optical potentials result in significant modifications to the response functions: Off-shell FSI are invariably important.

(2) The reactive content of the optical potentials, which is manifested in the energy dependence and non-Hermiticity of the optical potentials, is important to the description of the response functions. Hermitean, energy-independent potentials, such as the Hartree potential, fail to produce the appropriate shape for the response functions. This defect becomes more pronounced with increasing momentum transfer. Hermitean, energy-independent potentials transfer insufficient strength to the high-energy tails of the response functions. Energy-dependent, non-Hermitean optical potentials provide a much more realistic and physically appropriate analysis of quasielastic electron scattering.

(3) Since FSI suppress both R_L and R_T, the transverse response must be enhanced by physical mechanisms which are not included in the one-body optical model. This is supported by recent experimental and theoretical work in the $(e,e'p)$ reaction.[58,60] The transverse anomaly cannot be used to justify the plane-approximation nor should models which do not incorporate FSI suppression of the transverse response relative to the plane-wave result be considered advantageous.

(4) Relativistic negative-energy contributions, which are the new dynamical degrees of freedom included in the Dirac FSI, result in greater suppression of the longitudinal response than the transverse response. For the nonrelativistic FSI, the predicted suppression of the two response functions is roughly the same. Half of the additional "relativistic" suppression of the longitudinal quasielastic peak, and all of the additional "relativistic" suppression of the transverse peak, arises not from pair effects but from nonrelativistic-type off-shell differences in the optical potential. The effects of explicit and implicit negative-energy "pair" contributions are of approximately the same magnitude; both suppress the longitudinal response while the two contributions tend to cancel for the transverse response. Thus pair effects double the additional relativistic suppression of the longitudinal response, but have little impact on the transverse response. The negative-energy components of the bound-state wave functions have a negligible effect on the response functions.

(5) The longitudinal response functions calculated with relativistic dynamical FSI have the appropriate shape, but the suppression is inadequate to account for the available data. No parameter-free description of the FSI was found able to simultaneously describe existing experimental data for both the longitudinal and transverse quasielastic response functions.

ACKNOWLEDGMENTS

Support of the U.S. Department of Energy and the University of Maryland Computer Science Center for this research is gratefully acknowledged. We would also like to thank B. C. Clark and J. J. Kelly for the use of their optical potential models in our analyses.

APPENDIX A

This appendix extends the unsymmetrized formalism Eqs. (7)–(19) of the text to properly reflect the full implications of the Pauli principle. The purposes of this are (1) to provide a fully antisymmetrized formal development: (2) to show that all of the main results of the text, namely Eqs. (16)–(19), are consistent with the fully an-

tisymmetrized development; and [3] to point out some interesting theoretical points that arise as a result of the Pauli principle.

Given Eq. (9) we wish to connect the operator $P_{\alpha_i}\hat{G}P_{\alpha_i}$ to the optical theory as before. First the ejectile-nucleus antisymmetrization operator $\hat{A}$ is introduced, where $\hat{A}$ is a full A-particle antisymmetrizer normalized according to

$$\hat{A}^2 = A\hat{A} , \tag{A1}$$

so that

$$\Lambda = \hat{A}/A \tag{A2}$$

is the usual projection operator onto antisymmetric states

$$\Lambda^2 = \Lambda . \tag{A3}$$

The antisymmetrization requirement on $\hat{G}$ is made explicit in Eq. (9) by replacing

$$P_{\alpha_i}\hat{G}P_{\alpha_i} \text{ with } P_{\alpha_i}\Lambda\hat{G}P_{\alpha_i} , \tag{A4}$$

so that Eq, (9) becomes

$$T^{\mu\nu} \simeq \sum_i \sum_{\alpha_i} \langle i|\hat{J}^{\mu}(q)^{\dagger}P_{\alpha_i}\Lambda\hat{G}P_{\alpha_i}\hat{J}^{\nu}(q)|i\rangle . \tag{A5}$$

This follows, for example, by replacing $\hat{G}$ by $\Lambda\hat{G}$ in Eq. (5) and carrying it forward to Eq. (9). Now from the resolvent identity

$$\hat{G}\hat{A} = G_{\alpha_i}\hat{A} + G_{\alpha_i}V^{\alpha i}\hat{A}\hat{G} \tag{A6}$$

$$= G_{\alpha_i} + G_{\alpha_i}T^{\alpha i}_{\mathrm{AGS}}G_{\alpha_i} , \tag{A7}$$

where $T^{\alpha_i}_{\mathrm{AGS}}$ is the Alt-Grassberger-Sandhas (AGS) form of the antisymmetrized transition operator[61]

$$T^{\alpha_i}_{\mathrm{AGS}} = G^{-1}_{\alpha_i}\hat{G}\hat{A}G^{-1}_{\alpha_i} - G^{-1}_{\alpha_i} , \tag{A8a}$$

$$= V^{\alpha_i}\hat{A}\hat{G}G^{-1}_{\alpha_i} + (\hat{A}-1)G^{-1}_{\alpha_i} \tag{A8b}$$

If we now make the replacements (11) for (A6), (13) for (A8), we make use of the definitions (12) and (14), and replace $(1/A)\sum_{\alpha_i}$ for $\sum_{\alpha_i}$, where the latter sum runs over physically distinct channels, Eq. (16) is recovered where now $V^{\alpha_i}_{\mathrm{opt}}$ is the AGS-based optical potential of Refs. 36 and 37. It is not at all surprising that it is this optical potential which should arise here.[36,38] In fact, Eq. (A8a) is Hermitean analytic so that the associated optical potential is Hermitean analytic as well. Thus the unitarity and dispersion relations (17)–(19) are also recovered in the same form as in the text.

In contrast, the optical potential based on the more usual "prior" form of the antisymmetrized transition operator, which is just the first term on the right-hand side of (A8b), is not Hermitean analytic and hence neither is its associated optical potential. Because of this, discontinuity and unitarity relations do not coincide and relation (19) is not obeyed. This is of interest because the multiple scattering theoretic basis for high-energy approximations to the optical potential is derived on the basis of the prior form of the T matrix[39] (see, however, Ref. 38 for a multiple scattering series based on $T^{\alpha_i}_{\mathrm{AGS}}$).

It is interesting that the result of this appendix implies that, at least in principle, Eq. (16) requires the use of the optical potential based upon the AGS form for T, in distinction from other off-shell extensions of T. From Eqs. (A6)–(A8) this is connected to the spectral decomposition of $\hat{G}$ and thus to the Coulomb sum rule, as well as to the analytic structure of $V^{\alpha_i}_{\mathrm{opt}}$. Since the optical potential based on $T^{\alpha_i}_{\mathrm{AGS}}$ is free of the elastic α_i-channel unitary cut whereas the prior-based optical potential is not,[36–38] this dichotomy carries over at least formally to the Coulomb sum rule within the context of the one-body optical model.

[1] E. J. Moniz, Phys. Rev. **184**, 1154 (1969); A. L. Fetter and J. D. Walecka, *Quantum Theory of Many Particle Systems* (McGraw-Hill, New York, 1971), pp. 192–194.

[2] E. J. Moniz, *et al.*, Phys. Rev. Lett. **26**, 455 (1971); R. R. Whitney *et al.*, Phys. Rev. C **9**, 2230 (1974); J. W. Van Orden, Ph.D. thesis, Stanford University, 1978.

[3] Z. E. Meziani *et al.*, Phys. Rev. Lett. **52**, 2130 (1984); **54**, 1233 (1985); Nucl. Phys. **A46**, 113c (1985).

[4] M. Deady *et al.*, Phys. Rev. C **33**, 1897 (1986); **28**, 631 (1983).

[5] C. C. Blatchley *et al.*, Phys. Rev. C **34**, 1243 (1986); B. Frois, Nucl. Phys. **A434**, 57 (1985); A. Hotta *et al.*, Phys. Rev. C **30**, 87 (1984); P. Barreau *et al.*, Nucl. Phys. **A402**, 515 (1983); **A358**, 287c (1981); R. Altemus *et al.*, Phys. Rev. Lett. **44**, 965 (1980).

[6] U. Stroth, R. W. Hasse, and P. Schuck, Nucl. Phys. **A462**, 45 (1987); Phys. Lett. B **171**, 339 (1986); W. M. Alberico, A. Molineri, A. DePace, M. Ericson, and M. B. Johnson, Phys. Rev. C **34**, 977 (1986); F. A. Brieva and A. Dellafiore, *ibid.* **36**, 899 (1987); C. Co' and S. Krewald, Nucl. Phys. **A433**, 392 (1985); M. Cavinato *et al.*, *ibid.* **A423**, 376 (1984).

[7] S. Fantoni and V. R. Pandharipande, Nucl. Phys. **A473**, 234 (1987).

[8] W. M. Alberico, A. Molineri, A. De Pace, M. Ericson, and M. B. Johnson, Phys. Rev. C **34**, 977 (1986); J. Jaenicke, P. Schuck, and R. W. Hasse, Phys. Lett. B **214**, 1 (1988).

[9] G. Co', K. Quader, R. D. Smith, and J. Wambach, Nucl. Phys. **A485**, 61 (1988); G. Co', K. Quader, and J. Wambach, Proceedings of the Second Workshop on Problems of Theoretical Nuclear Physics, Cortona, Italy, 1987 [University of Illinois Report No. Ill-(NU)-87-58, (1987)]; S. Drożdż, G. Co', J. Wambach, and J. Speth, Phys. Lett. B **185**, 287 (1987).

[10] G. Do Dang, M. L'Huillier, N. Van Giai, and J. W. Van Orden, Phys. Rev. C **35**, 1637 (1987); G. Orlandini and M. Traini, *ibid.* **31**, 280 (1985); see also Ref. 4.

[11] H. Kurasawa and T. Suzuki, Phys. Lett. B **208**, 160 (1988); **211**, 500(E) (1988); J. V. Noble, *ibid.* **178**, 285 (1986); Phys. Rev. Lett. **46**, 412 (1981); L. S. Celenza, A. Rosenthal, and C. M. Shakin, *ibid.* **53**, 892 (1984); Phys. Rev. C **31**, 232 (1985).

[12] P. J. Mulders, Phys. Rev. Lett. **54**, 2560 (1985); Nucl. Phys. **A459**, 525 (1986).

[13] R. Rosenfelder, Ann. Phys. (N.Y.) **128**, 188 (1980).

[14] G. Do Dang and Nguyen Van Giai, Phys. Rev. C **30**, 731

(1984); S. Nashizaki, H. Kurasawa, and Toshio Suzuki, Phys. Lett. B **171**, 1 (1986); S. Nishizaki, T. Maruyama, H. Kurasawa, and T. Suzuki, Nucl. Phys. **A485**, 515 (1988).

[15]R. Brockmann, private communication.

[16]K. Wehrberger and F. Beck, Phys. Rev. C **35**, 298 (1987); **37**, 1148 (1988).

[17]H. Kurasawa and T. Suzuki, Nucl. Phys. **A454**, 527 (1986); Kyoto University Report No. RIFP-739; MIT Report No. CTP-1589; MIT Report No. CTP-1601.

[18]C. J. Horowitz, Indiana University Report No. IU/NTC 88-4; in *Proceedings of the Workshop on Relativistic Nuclear Many-Body Physics, Columbus, 1988,* edited by B. C. Clark, R. J. Perry, and J. P. Vary (World Scientific, Singapore, 1989); C. J. Horowitz and J. Pickarewicz, Phys. Rev. Lett. **62**, 391 (1989).

[19]J. R. Shepard, in *Proceedings of the Workshop on Relativistic Nuclear Many-Body Physics, Columbus, 1988,* edited by B. C. Clark, R. J. Perry, and J. P. Vary (World Scientific, Singapore, 1989); J. R. Shepard, E. Rost, and J. A. McNeil, submitted to Phys. Rev. C.

[20]Xiangdong Ji, Phys. Lett. B **219**, 143 (1989).

[21]J. D. Walecka, Ann. Phys. (N.Y.) **83**, 491 (1974).

[22]R. J. Furnstahl, R. J. Perry, and B. D. Serot, Indiana University Report No. IU/NTC 88-18, 1989.

[23]T. D. Cohen, M. K. Banerjee, and C. Y. Ren, Phys. Rev. C **36**, 1653 (1987).

[24]Y. Kawazoe, G. Takeda, and H. Matsuzaki, Prog. Theor. Phys. **54**, 1394 (1975); S. Klawansky *et al.*, Phys. Rev. C **7**, 795 (1973); T. W. Donnelly, Nucl. Phys. **A150**, 393 (1970); T. de Forest, Jr., *ibid.* **A132**, 305 (1969).

[25]Y. Horikawa, F. Lenz, and Nimai C. Mukhopadhyay, Phys. Rev. C **22**, 1680 (1980).

[26]J. J. Kelly *et al.*, Phys. Rev. C (to be published); J. J. Kelly, in *Complementarity Between Electromagnetic and Hadronic Probes of Nuclear Structure,* Proceedings of the Conference on Critical Relationship between Structure and Reactions in Nuclear Physics, Philadelphia, 1986, edited by T. H. Feng, M. Vallieres, and B. H. Wildenthal (World Scientific, Singapore, 1987), p. 222.

[27]H. Feshbach, Ann. Phys. (N.Y.) **5**, 357 (1958); **19**, 287 (1962).

[28]P. Schwandt *et al.*, Phys. Rev. C **26**, 55 (1982).

[29]K. Nakayama and W. G. Love, Phys. Rev. C **38**, 51 (1988).

[30]A. Picklesimer, P. C. Tandy, R. M. Thaler, and D. H. Wolfe, Phys. Rev. C **29**, 1582 (1984); **30**, 1861 (1984).

[31]M. V. Hynes, A. Picklesimer, P. C. Tandy, and R. M. Thaler, Phys. Lett. **52**, 978 (1984); Phys. Rev. C **31**, 1438 (1985).

[32]See, for example, H. Feshbach, Annu. Rev. Nucl. Sci. **8**, 49 (1958); Ref. 27; and Ref. 36.

[33]See, for example, P. Schwandt, F. Petrovich, and A. Picklesimer, Indiana University Cyclotron Facility report, 1978, p. 27.

[34]J. A. McNeil, J. R. Shepard, and S. J. Wallace, Phys. Rev. Lett. **50**, 1429 (1983); J. R. Shepard, J. A. McNeil, and S. J. Wallace, *ibid.* **50**, 1443 (1983); B. C. Clark, S. Hama, R. L. Mercer, L. Ray, and B. D. Serot, *ibid.* **50**, 1644 (1983).

[35]E. D. Cooper *et al.*, Phys. Rev. C **36**, 2170 (1987); E. D. Cooper, B. C. Clark, S. Hama, and R. L. Mercer, Phys. Lett. B **206**, 588 (1988); **220**, 658(e) (1989).

[36]K. L. Kowalski and A. Picklesimer, Phys. Rev. Lett. **46**, 228 (1981); Nucl. Phys. **A369**, 336 (1981).

[37]R. Goldflam and K. L. Kowalski, Phys. Rev. Lett. **44**, 1044 (1980); Phys. Rev. C **22**, 949 (1980).

[38]A. Picklesimer, Phys. Rev. C **24**, 1400 (1981).

[39]E. R. Siciliano and R. M. Thaler, Phys. Rev. C **16**, 1322 (1977); A. Picklesimer and R. M. Thaler, *ibid.* **23**, 42 (1981).

[40]T. de Forest, Jr. and J. D. Walecka, Adv. Phys. **15**, 1 (1966); T. W. Donnelly and J. D. Walecka, Annu. Rev. Nucl. Sci. **25**, 729 (1975).

[41]J. D. Bjorken and S. D. Drell, *Relativistic Quantum Mechanics* (McGraw-Hill, New York, 1964).

[42]More generally, the simplification introduced by Eq. (8) is not needed for this result.

[43]Formally, this assumes that the optical potential is Hermitean analytic.

[44]A. Picklesimer, J. W. Van Orden, and S. J. Wallace, Phys. Rev. C **32**, 1312 (1985).

[45]See, for example, P. Stichel and E. Werner, Nucl. Phys. **A145**, 257 (1970); M. Chemtob and M. Rho, *ibid.* **A163**, 1 (1971); M. Gari and H. Hyuga, Z. Phys. A **277**, 291 (1976); W. Jaus and W. Woolcock, Nucl. Phys. **A431**, 669 (1984); J. L. Friar and W. C. Haxton, Phys. Rev. C **31**, 2027 (1985); W. M. Alberico, R. Cenni, A. Molinari, and P. Saracco, Ann. Phys. (N.Y.) **174**, 131 (1987).

[46]A. J. F. Siegert, Phys. Rev. **52**, 787 (1937); J. L. Friar and S. Fallieros, Phys. Lett. **114B**, 403 (1982); Phys. Rev. C **29**, 1645 (1984).

[47]See, for example, A. Gal, G. Toker, and Y. Alexander, Ann. Phys. (N.Y.) **137**, 341 (1981).

[48]M. Kohno and N. Ohtsuka, Phys. Lett. **98B**, 335 (1981).

[49]P. G. Blunden and M. N. Butler, TRIUMF report, 1988.

[50]J. W. Van Orden and T. W. Donnelly, Ann. Phys. (N.Y.) **131**, 451 (1981).

[51]A. Fabrocini and F. Fantoni, University of Pisa Report No. IFUP-2H36/88, 1988.

[52]M. N. Butler and S. E. Koonin, Phys. Lett. B **205**, 123 (1988).

[53]C. J. Horowitz and B. D. Serot, Nucl. Phys. **A368**, 503 (1981).

[54]G. Höhler *et al.*, Nucl. Phys. **B114**, 505 (1976).

[55]J. L. Friar, private communication.

[56]C. R. Chinn, A. Picklesimer, and J. W. Van Orden, Phys. Rev. C (to be published).

[57]M. A. Franey and W. G. Love, Phys. Rev. C **31**, 488 (1985).

[58]See also, P. E. Ulmer *et al.*, Phys. Rev. Lett. **59**, 2259 (1987).

[59]A. Dellafiore, F. Lenz, and F. A. Brieva, Phys. Rev. C **31**, 1088 (1985); see also Ref. 25.

[60]A. Picklesimer and J. W. Van Orden, Phys. Rev. C **40**, 290 (1989).

[61]E. O. Alt, P. Grassberger, and W. Sandhas, Nucl. Phys. **B2**, 167 (1967); P. Grassberger and W. Sandhas, *ibid.* **B2**, 181 (1967).